# Supporting Information

# for

# Synthesis of dynamic *N*-acylhydrazone-based macrocycles

Nicoleta Sandu,[a,§] Anamaria Hanganu,[a,b,§] Codruța Popescu,[a,§] Alexandra M. Demeter,[c] Anca G. Mirea,[d] Andrei Kuncser,[d] Cristina Tablet,[e] Niculina D. Hădade, [f] Mihaela Florea,[d,g] Daniel P. Funeriu*[,a] and Mihaela Matache*[,a]

[a] University of Bucharest, Faculty of Chemistry, Research Centre of Applied Organic Chemistry, 90 Panduri Street, RO-050663 Bucharest, Romania. E-mail: mihaela.matache@g.unibuc.ro (M. Matache)

[b] "C. D. Nenitzescu" Institute of Organic and Supramolecular Chemistry of the Romanian Academy, 202B Spl. Independenței, 060023 Bucharest, Romania

[c] SC Microsin SRL, Department of Research and Development, 51-63 Pericle Papahagi Street, 032364 Bucharest, Romania

[d] National Institute of Materials Physics, 405A Atomistilor Street, 077125, Magurele, Romania

[e] Titu Maiorescu University, Faculty of Pharmacy, Gh. Sincai Bd. 16, 040317 Bucharest, Romania

[f] Faculty of Chemistry and Chemical Engineering, Supramolecular Organic and Organometallic Chemistry Centre, ''Babes-Bolyai'' University, 11 Arany Janos Str., 400028, Cluj-Napoca, Romania.

[g] University of Bucharest, International School of Doctoral Studies, 90 Panduri Street, RO-050663 Bucharest, Romania.

[§] These authors contributed equally

# Contents

# 1. Organic synthesis

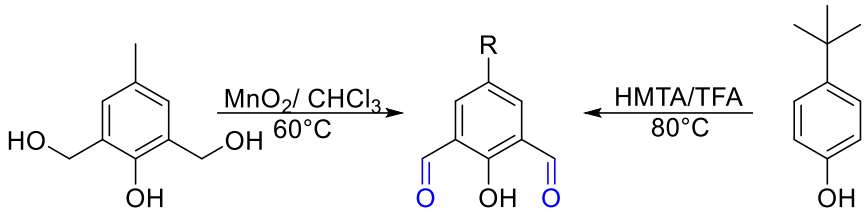


1a: R = Me; η = 90 %
1b: R = t-Bu; η = 57%

Scheme S 1 Synthesis of aldehydes **1a,b**

**5-methyl-2-hydroxybenzen-1,3-dialdehyde** (**1a**)[1]. In a round bottom flask 2,6-bis(hydroxymethyl)-4-cresol (59.5 mmol, 1 eq.) and $CHCl_3$ (100 mL) were added. The mixture was stirred at room temperature until complete dissolution and activated $MnO_2$ (1.2 mmol, 20 eq.) was added. The mixture was heated at 60°C until the raw material was consumed (24 h). The reaction mixture was filtered on celite, the solvent was evaporated, isolating an impure yellow solid. The compound was purified through recrystallisation MeOH/$H_2O$. Yellow solid. Yield 90 %. *m.p.* 129-132°C (lit. 129-130°C[2]). $R_f$ = 0.69 (AcOEt : Petroleum Ether = 3 : 1). $^1$H RMN (500 MHz, $CDCl_3$): δ=11.45 (s, 1H, O*H*); 10.21 (s, 2H, C*H*O); 7.77 (s, 2H, $H_{aromatic}$); 2.38 (s, 3 H, $CH_3$) ppm. $^{13}$C RMN (125 MHz, $CDCl_3$): δ=192.2; 161.8; 138.0; 129.5; 122.9; 20.1 ppm. $^1$H RMN (500 MHz, DMSO-$d_6$): δ=11.40 (s, 1H, O*H*); 10.22 (s, 2H, C*H*O); 7.86 (s, 2H, $H_{aromatic}$); 2.34 (s, 3 H, $CH_3$) ppm.

**5-(*tert*-butyl)-2-hydroxybenzen-1,3-dialdehyde** (**1b**)[3]. 4-hydroxybenzoic acid (36.2 mmol, 1 eq.), HMTA (hexamethylentetramine, 111.2 mmol, 4 eq.) and TFA (trifluoroacetic acid, 29 mL, 14 eq.) were added to a round bottom flask. The mixture was heated at 80°C until raw material was consumed. Water (100 mL) was added to the reaction mixture and heated at 80°C until a yellow solid formed. The mixture was cooled, filtered under vacuum and the precipitate was rinsed with water and dried. The compound was purified through column chromatography with silica gel as a stationary phase, and the mobile phase was a volumetric mixture of AcOEt : Petroleum Ether = 1:20. After the purification step, a straw yellow solid was obtained Yellow solid. Yield 57%. *m.p.* 108-110°C (lit. 104-105°C[2]). $R_f$ = 0.68 (AcOEt : Petroleum Ether = 1 : 10). $^1$H RMN (300 MHz, $CDCl_3$): δ=11.48 (s, 1H, O*H*); 10.24 (s, 2H, C*H*O); 7.98 (s, 2H, $H_{aromatic}$); 1.35 (s, 9 H, t-Bu) ppm. $^{13}$C RMN (75 MHz, $CDCl_3$): δ=192.4; 161.7; 143.1; 134.7; 123.6; 122.7; 34.3; 31.1 ppm. $^1$H RMN (500 MHz, DMSO-$d_6$): δ=11.45 (s, 1H, O*H*); 10.25 (s, 2H, C*H*O); 8.09 (s, 2H, $H_{aromatic}$); 1.31 (s, 9 H, *t*-Bu) ppm.

**Dimethylterephthalate.** Benzen-1,4-dioic acid (18.1 mmol, 1 eq.) and 90 mL MeOH were added to a round bottomed flask. When the acid had dissolved, $SOCl_2$ (thionyl chloride, 15 mL, 12 eq.) was gradually added dropwise. The mixture was heated at 60°C. After the raw material was consumed, the reaction mixture was diluted with water (60 mL). The compound was extracted in ethyl ether (3 x 150 mL). The organic phase was mixed, rinsed with saturated solution of sodium bicarbonate (600 mL), traces of water were removed with anhydrous magnesium sulphate and the solvent was evaporated by rotary evaporator, to afford the pure compound. White solid. Yield 93% (3.25 g). *m.p.* 142 – 145°C (140.72°C[4], 139-141°C[5]). $R_f$ = 0.78 (AcOEt : Petroleum Ether = 1 : 2). $^1$H RMN (500 MHz, $CDCl_3$): δ=8.10 (s, 4H, $H_{aromatic}$); 3.95 (s, 6 H, $CH_3O$) ppm. $^{13}$C RMN (125 MHz, $CDCl_3$): δ=166.3; 133.9; 129.6; 52.4 ppm.

**1,4-Benzendihydrazide** (**2c**). Diethylterephthalate (1.51 mmol, 1 eq.) and MeOH (60 mL) were added to a round bottomed flask and the solution was heated to reflux. When the ester had dissolved in solvent,

hydrazine hydrate (11.5 mL, 7.5 eq.) was added. The reaction took place at reflux until the raw material was consumed. Over time, a white solid formed because the target compound is not soluble in reaction medium. The reaction mixture was filtered under reduced pressure, and the isolated precipitate was well rinsed with plenty of water to remove traces of hydrazine. The compound was purified through recrystallization from MeOH. White solid. Yield 73% (2,3 g). *m.p.* 320°C (decomposition; 310°C[6], 320°C[7]). $R_f$ = 0.44 (MeOH : DCM = 1 : 40).$^1$H RMN (500 MHz, DMSO-$d_6$): δ=9.87 (s, 2H, NH); 7.86 (s, 2H, $H_{aromatic}$); 4.53 (s, 4 H, $NH_2$) ppm.$^{13}$C RMN (125 MHz, DMSO-$d_6$): δ=165.1; 135.5; 126.9 ppm.

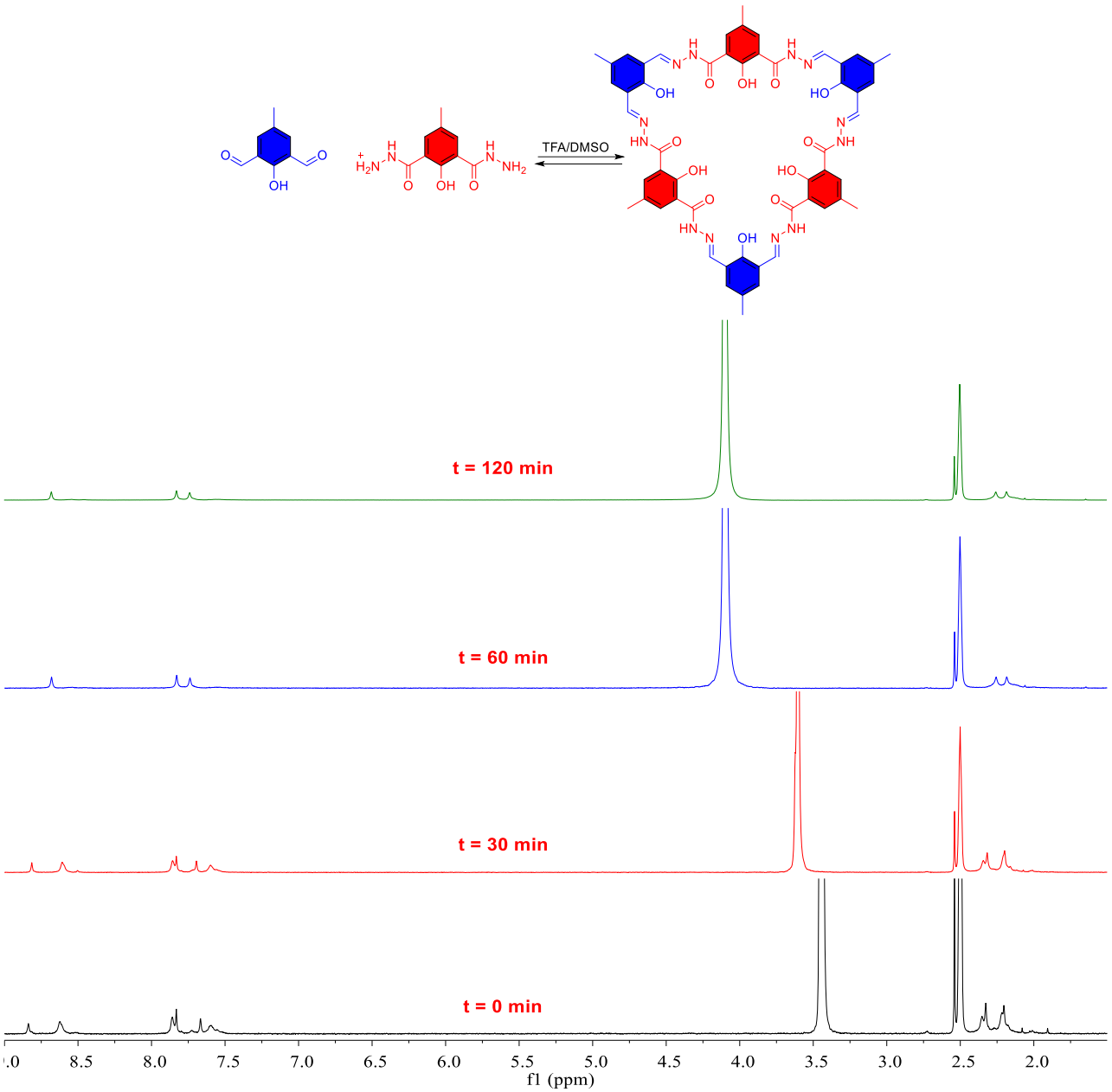


Figure S 1 $^1$H NMR spectra (fragments, 300 MHz, DMSO-$d_6$) in time of mixture of aldehyde **1a** and hydrazide **2a** (5 mM)

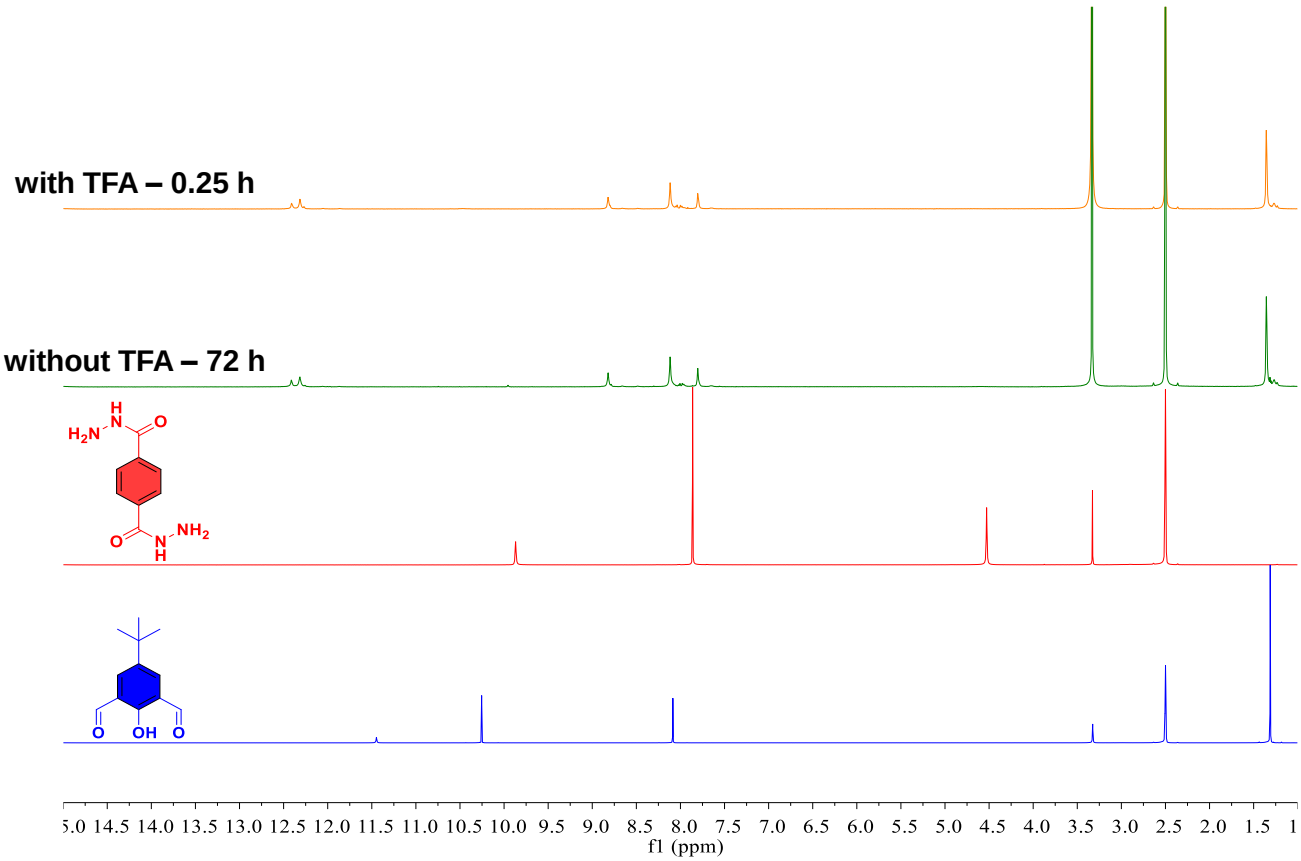


Figure S 2 $^{1}$H NMR spectra (500 MHz, DMSO-d6) recorded to monitor the evolution of the reaction between aldehyde **1b** and hydrazide **2c** (10 mM) performed in the NMR tube with and without acid catalyst

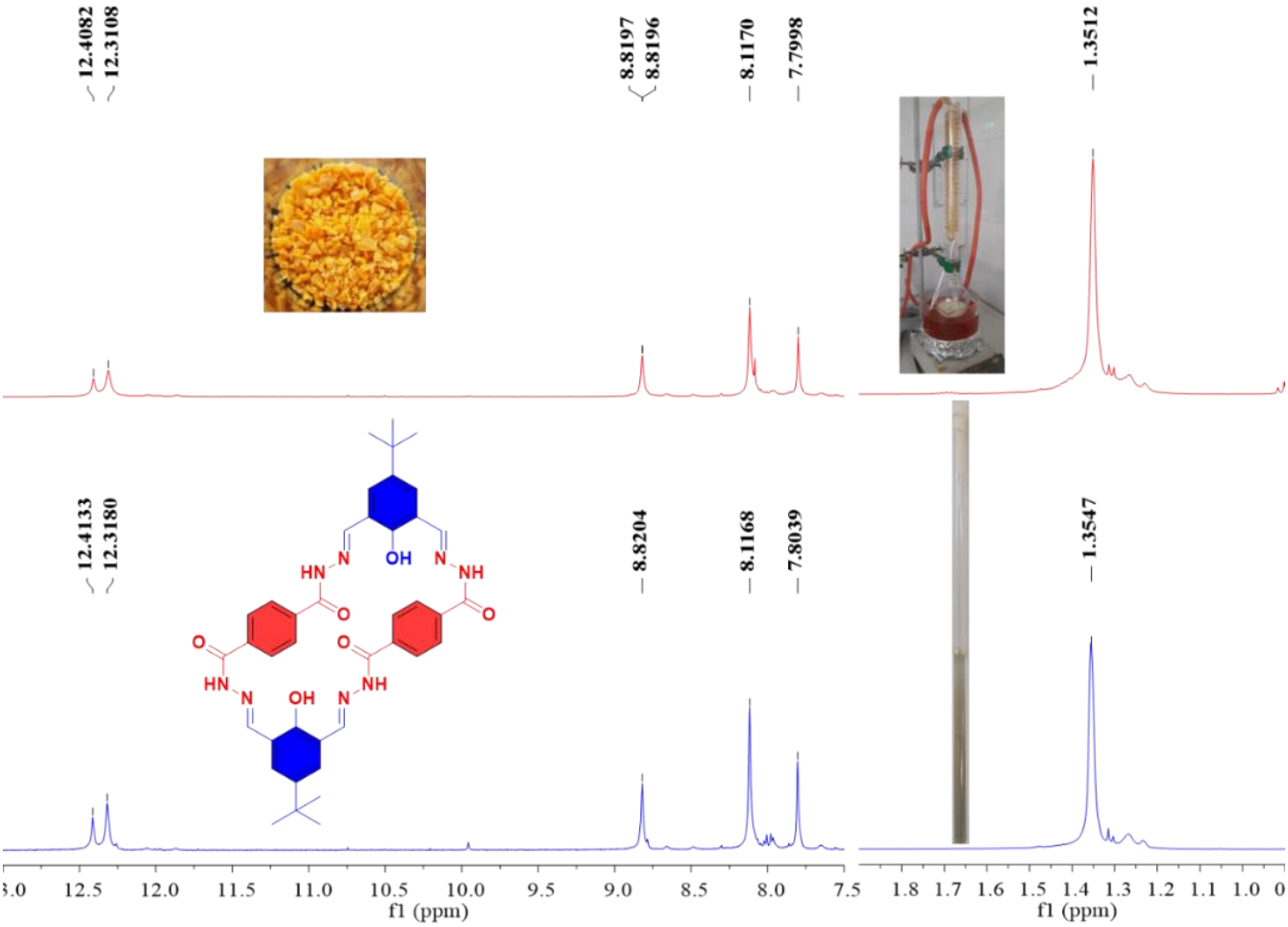


Figure S 3 $^{1}$H NMR spectra (fragments, 500 MHz, DMSO-$d_6$) of macrocycle **7** performed in NMR tube (bottom) and on larger scale and isolated (top)

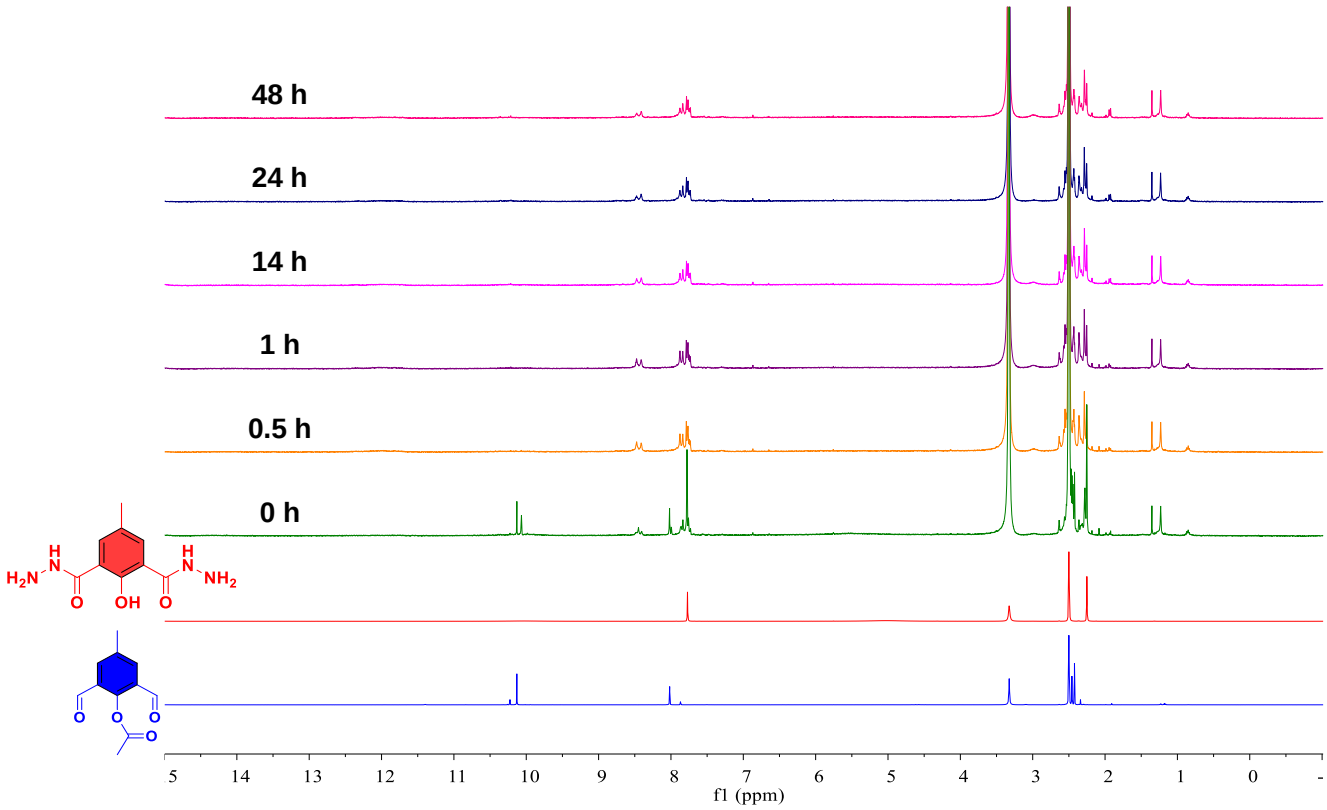


Figure S 4 $^{1}$H NMR spectra (500 MHz, DMSO-$d_6$) recorded to monitor the evolution of the reaction between aldehyde **1c** and hydrazide **2a** performed in the NMR tube

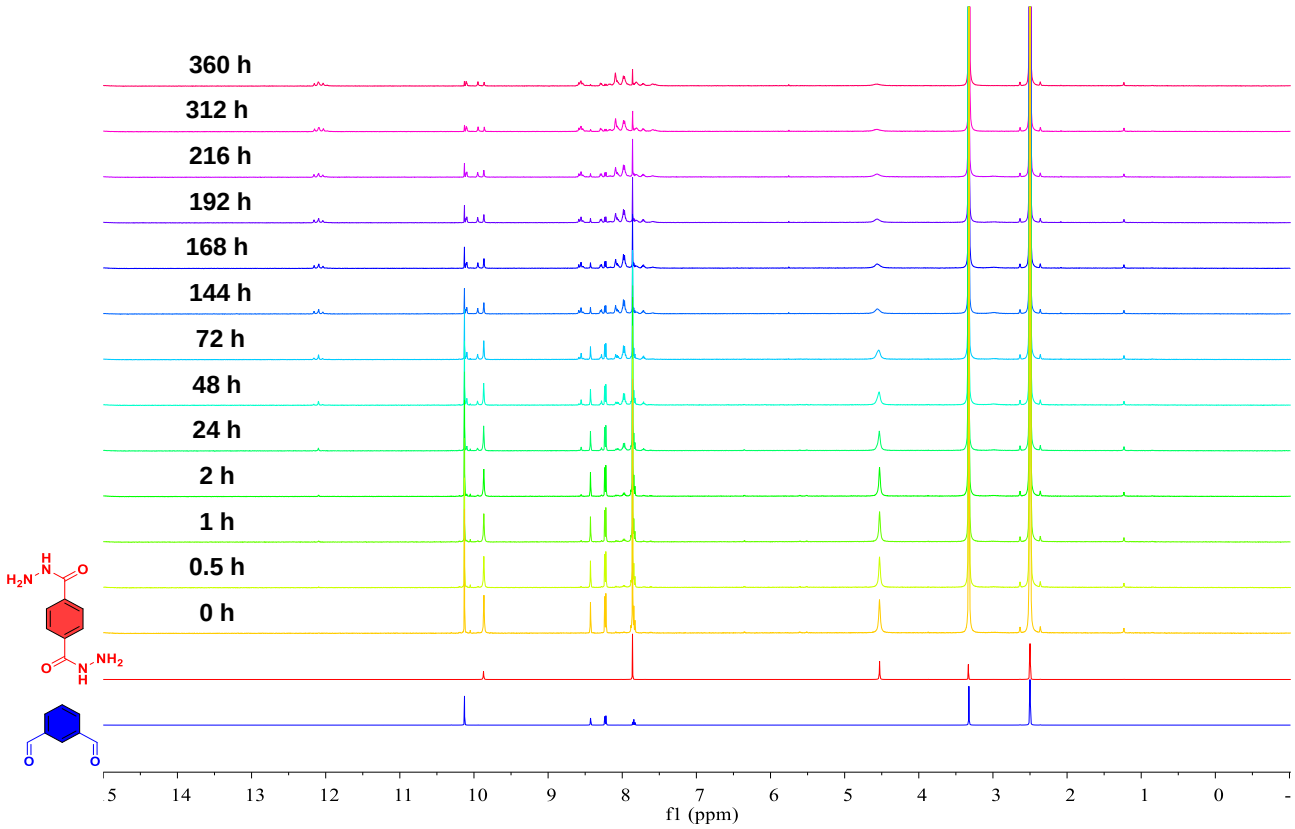


Figure S 5 $^{1}$H NMR spectra (500 MHz, DMSO-$d_6$) recorded to monitor the evolution of the reaction between aldehyde **3** and hydrazide **2c** performed in the NMR tube

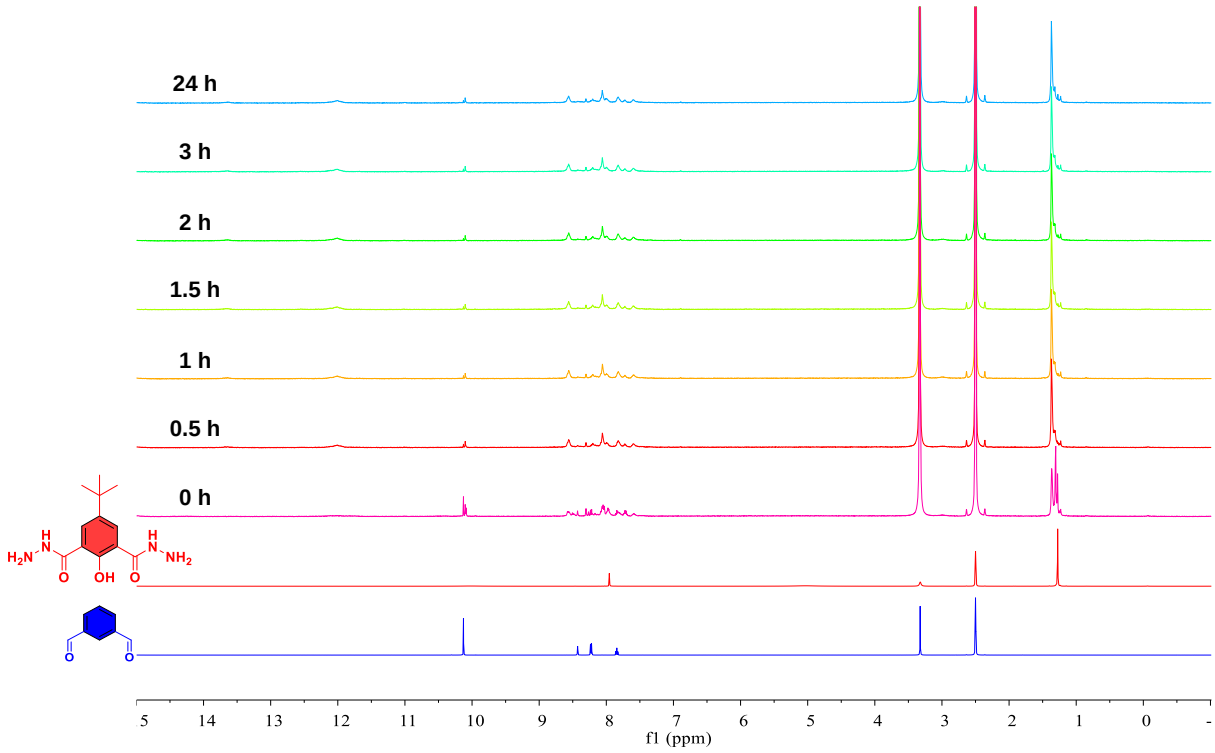


Figure S 6 $^{1}$H NMR spectra (500 MHz, DMSO-$d_6$) recorded to monitor the evolution of the reaction between aldehyde **3** and hydrazide **2b** performed in the NMR tube

## 2. DFT calculation

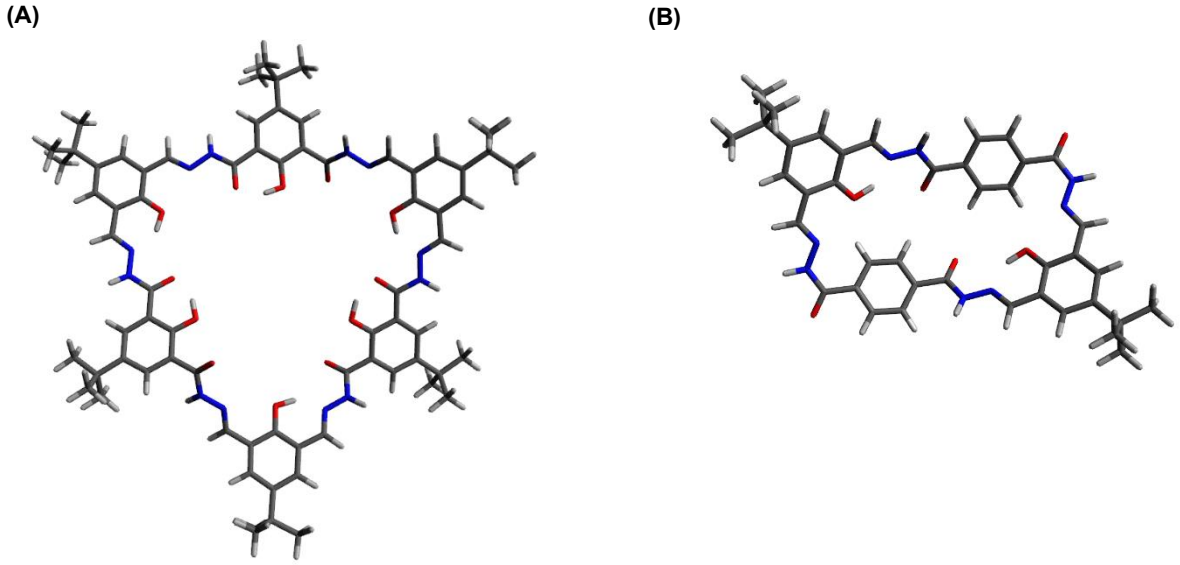


Figure S 7 Optimized structures of compounds **6** (A) and **7** (B).

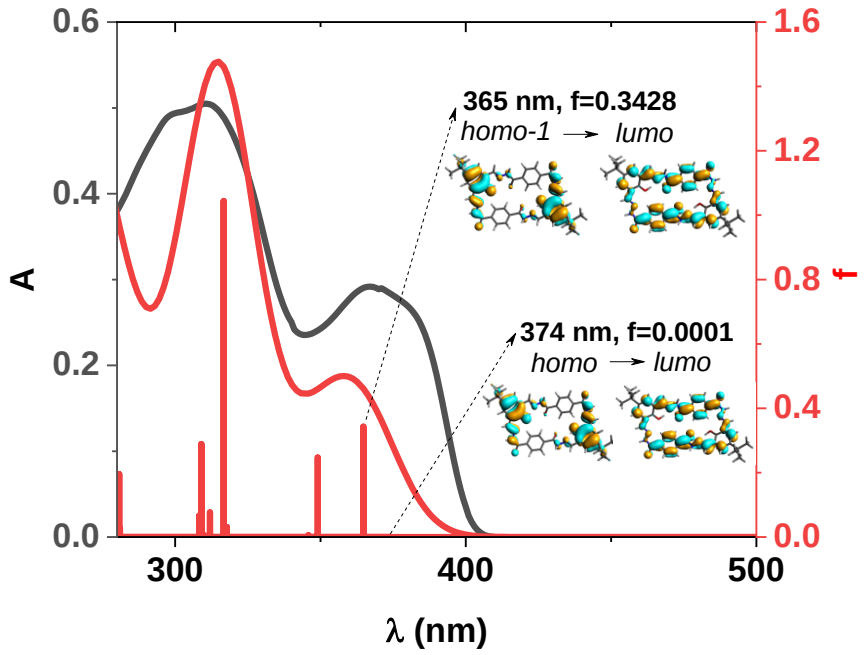


Figure S 8 Experimental vs. calculated (PBE0/6-31G(d)) absorption spectrum of **7** (neutral) in DMSO.

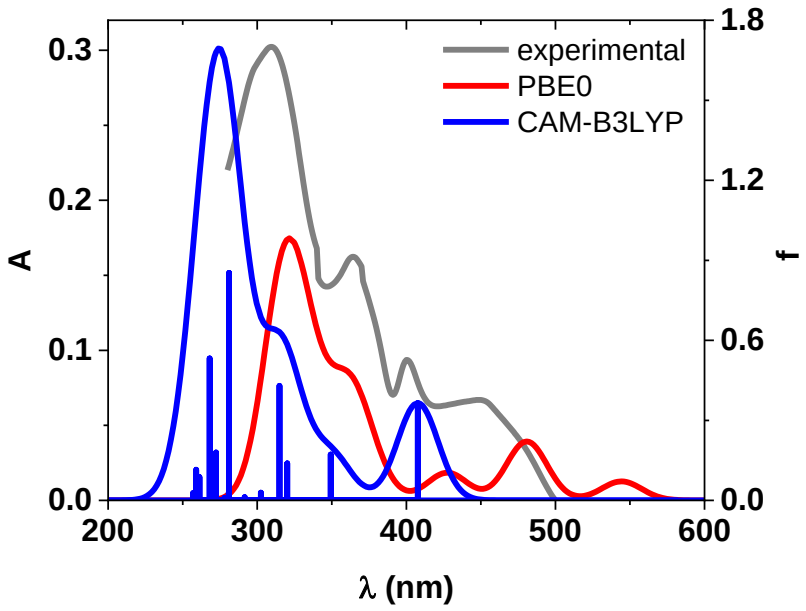


Figure S 9 Experimental absorption spectrum of **7** in presence of TBAF vs. calculated (6-31+G(d)) spectrum of **7** (monoanion) in DMSO.

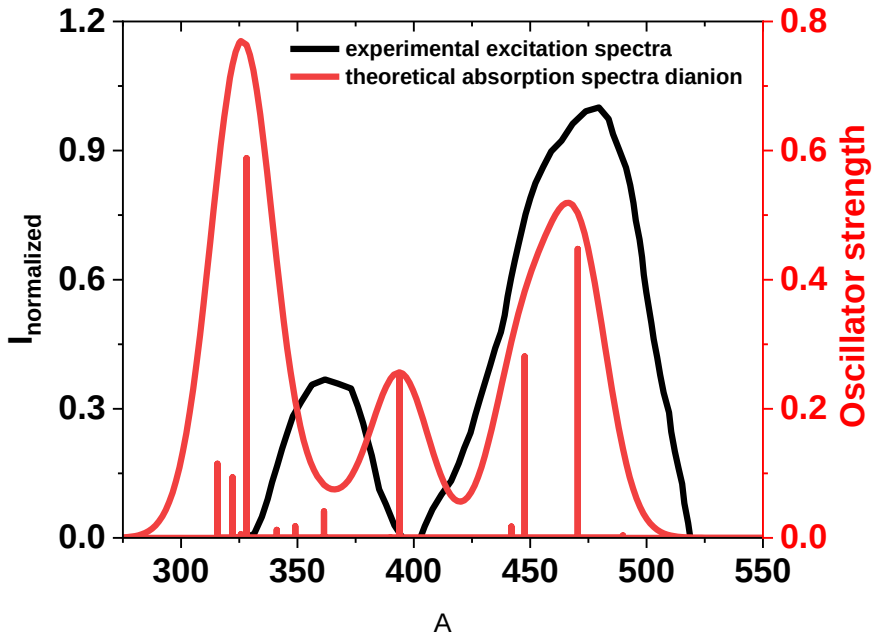


Figure S 10 Experimental excitation spectra of **7** and calculated (PBE0/6-31+G(d)) absorption spectrum of **7** (dianion) in DMSO.

# 3. FTIR spectroscopy

FTIR spectra of compounds **6** and **7** confirmed the presence of the hydrazone linkages. The peaks observed at ~1650 $cm^{-1}$ and ~1550 $cm^{-1}$ were assigned to $\nu_{(C=O)}$ and $\nu_{(C=N)}$ vibrational modes, respectively. Additionally, stretching vibrations at around 1220 $cm^{-1}$ are characteristic to $\nu_{(C=N)}$ moieties. The broad absorption band visible at ~3200 $cm^{-1}$ was assigned to $\nu_{(OH)}$ vibration mode.

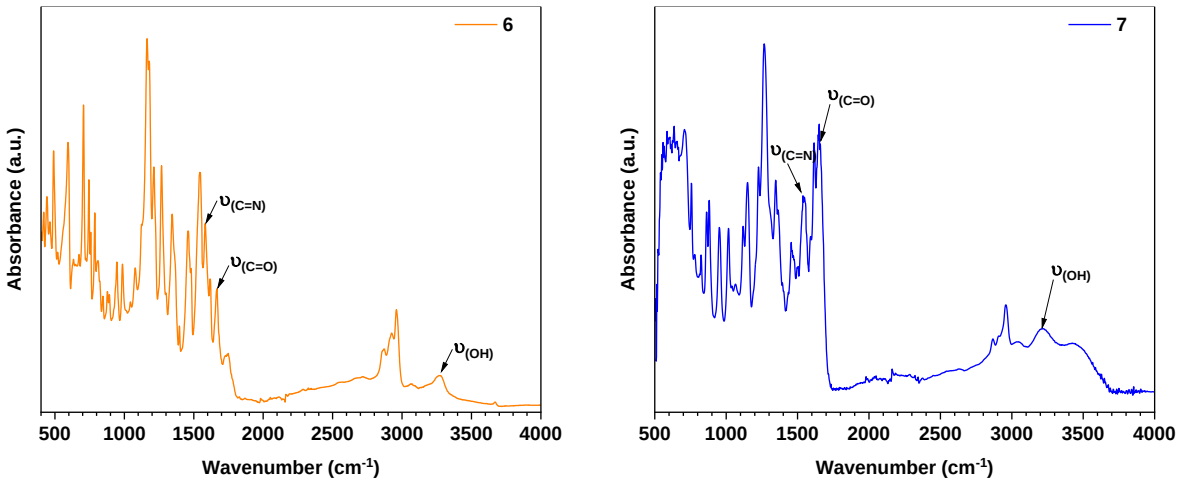


Figure S 11 FTIR spectra for compounds **6** (left) and **7** (right)

# 4. Thermogravimetry

The observed weight losses could be associated with elimination of species such as adsorbed water, surface OH groups, solvents, or even decomposition. The two compounds present different decomposition steps and weight losses. For compound **7** a slight weight loss (~2%) occurs up to 100 °C, likely due to water removal. This is followed by a 10% weight loss up to 200 °C, attributed to residual organic solvents from synthesis. Multiple steps suggest that water and solvent molecules have varying binding energies within the crystal lattice. The material remains stable up to approximately 350 °C. Beyond this temperature, a significant weight loss (~75%) is observed, likely due to decomposition processes associated with an exothermic process. For compound **6** a minor weight loss (~5%) is observed up to 315 °C, likely due to water or solvent elimination, associated with an endothermic process. Between 315 °C and 370 °C, a further 14% weight loss occurs, accompanied by an exothermic process. The total mass loss (~22%) up to 500 °C indicates higher stability compared to compound **7**, suggesting a more compact structure with stronger intermolecular interactions.

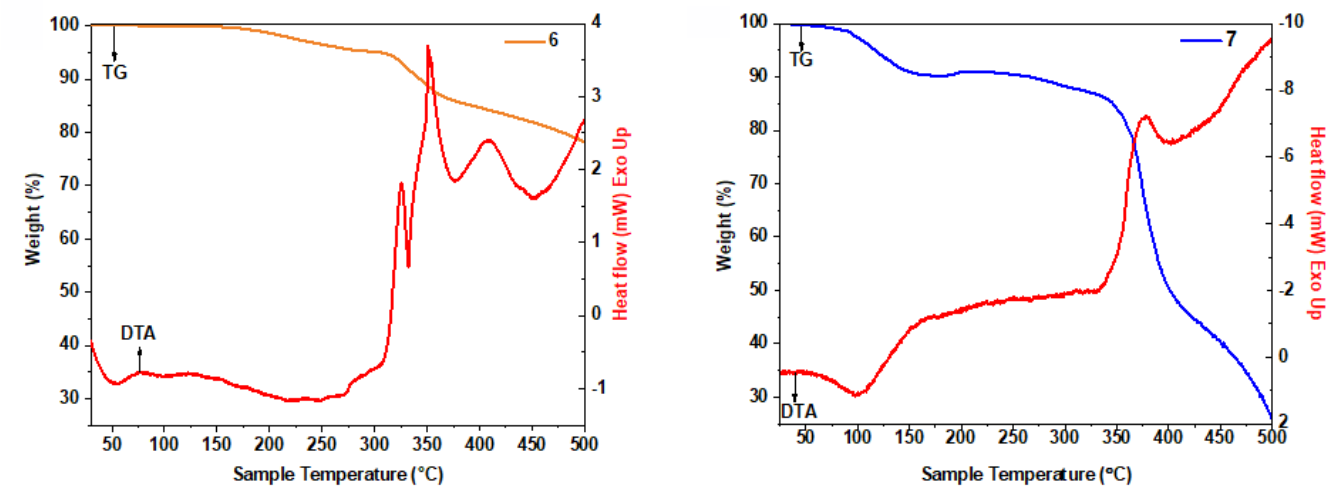


Figure S 12 Thermogravimetric measurements for **6** and **7**

# 5. SEM & TEM

According to SEM images, compound **7** presents a layered morphology, while **6** has a texture that is much more compact consistent with the thermogravimetric analysis indicating higher stability. Moreover, TEM images of **7** revealed once again the layered morphology of this compound.

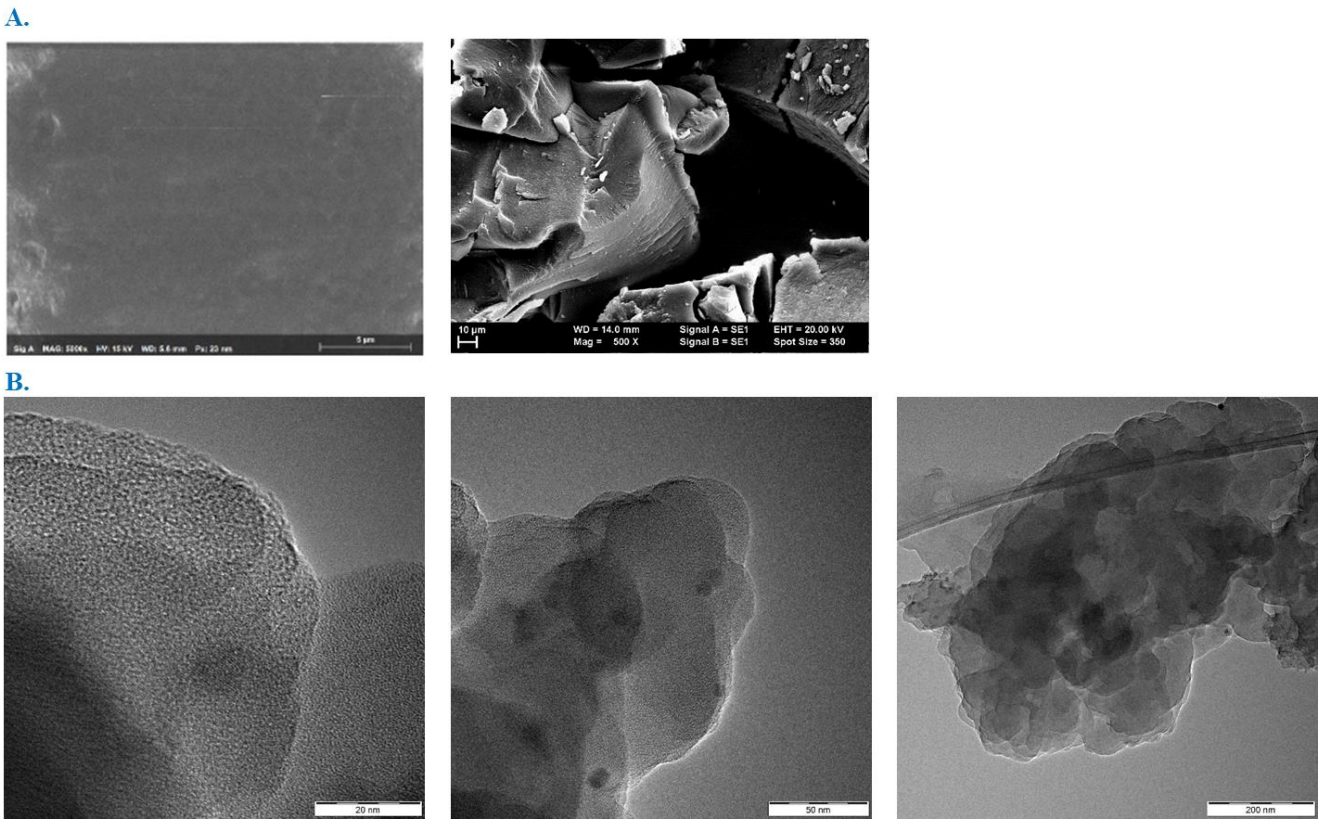


Figure S 13 **A.** SEM images of compounds **6** (left) and **7** (right). B. TEM images of compound **7** at different magnifications

# 6. PXRD

For compound **7** full-range PXRD patterns display three reflections with d-spacings of 4.7 Å, 3.5 Å, and 2.1 Å. Small-angle XRD patterns reveal additional reflections with d-spacings of 30.3 Å and 12.9 Å.

Compound **6 e**xhibits higher crystallinity, with an intense peak at 13.9 Å and additional peaks at 12.1 Å, 9.1 Å, 8.1 Å, 6.7 Å, 4.9 Å, and 3.4 Å.

The reflections corresponding to an interlayer *d*-spacing of 3.5 Å (for **7**) and 3.4 Å (for **6**), respectively, could be assigned to the distance of π-π stacking and could be attributed to the intra-columnar spacing between the parallel macrocyclic cores, Comparing the crystallite size of the two compounds calculated using Scherer equation we could observe that compound **7** had a smaller crystallite size (~35.5 Å) than compound **6** (~67.8 Å). Using the d-spacing between two macrocyclic cores and the crystallite size we were able to calculate the number of stacked macrocycles. Therefore, for compound **7** we have ~10 continuously stacked macrocycles, while for compound **6** there are ~20 stacked macrocycles.

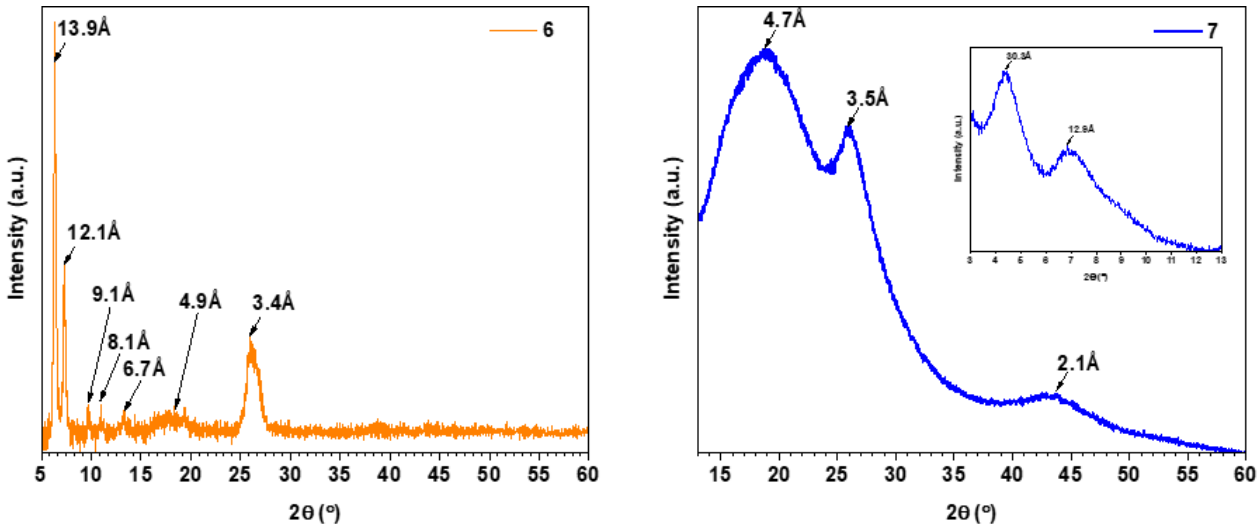


Figure S 14 XRD patterns of compound **6** and **7**

# 7. Absorption and emission spectroscopy

To determine the molar absorptivity (ε), several dilutions were performed within the concentration range $5 \cdot 10^{-6}$ – $5 \cdot 10^{-5}$ M. and we determined for $\lambda_{max}$ = 366 nm a value of ε = 39581 $L \cdot mol^{-1} \cdot cm^{-1}$.

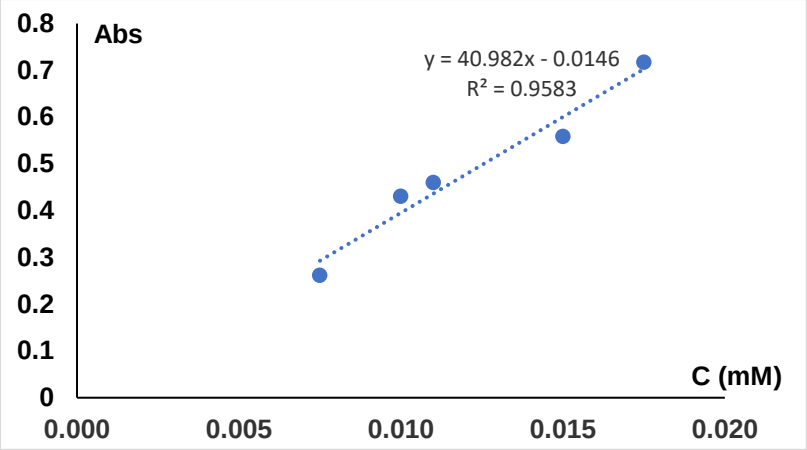


Figure S 15 Linear regression for determination of the molar absorption coefficient of compound **7**

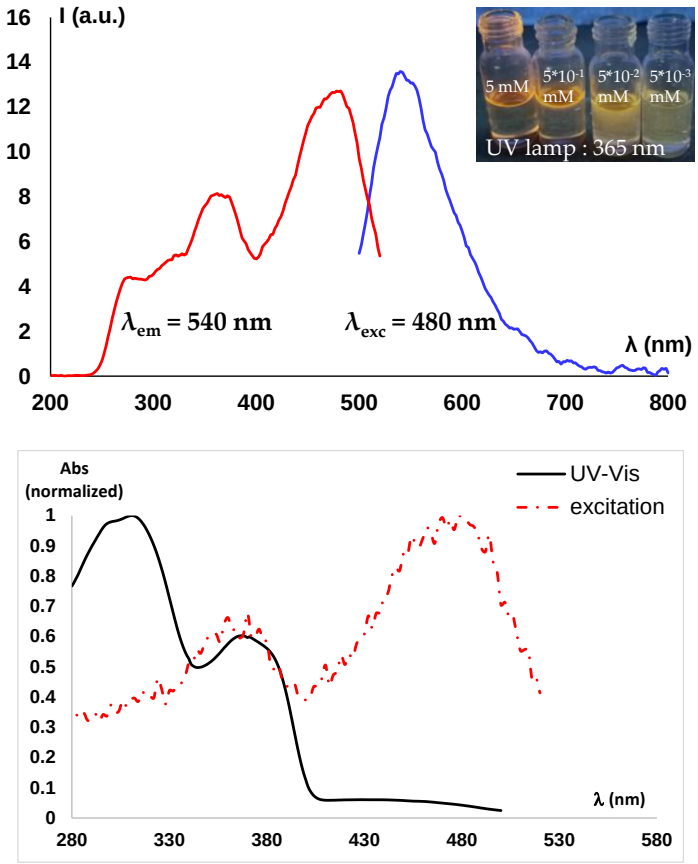


Figure S 16 **Top**: Excitation and emission spectra of compound 7 in DMSO; **Bottom**: Normalized absorption and excitation spectra of compound 7 in DMSO

# 8. Anion-complexation assays

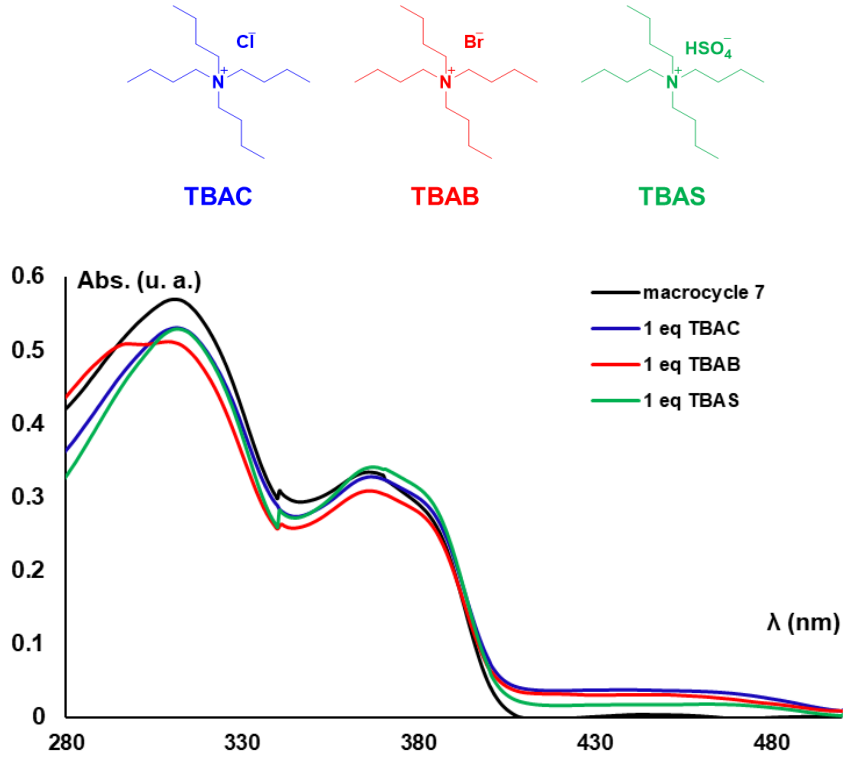


Figure S 17 UV-Vis absorption spectra of macrocycle **7** and mixture of macrocycle in presence of: blue – TBAC; red – TBAB; green – TBAS

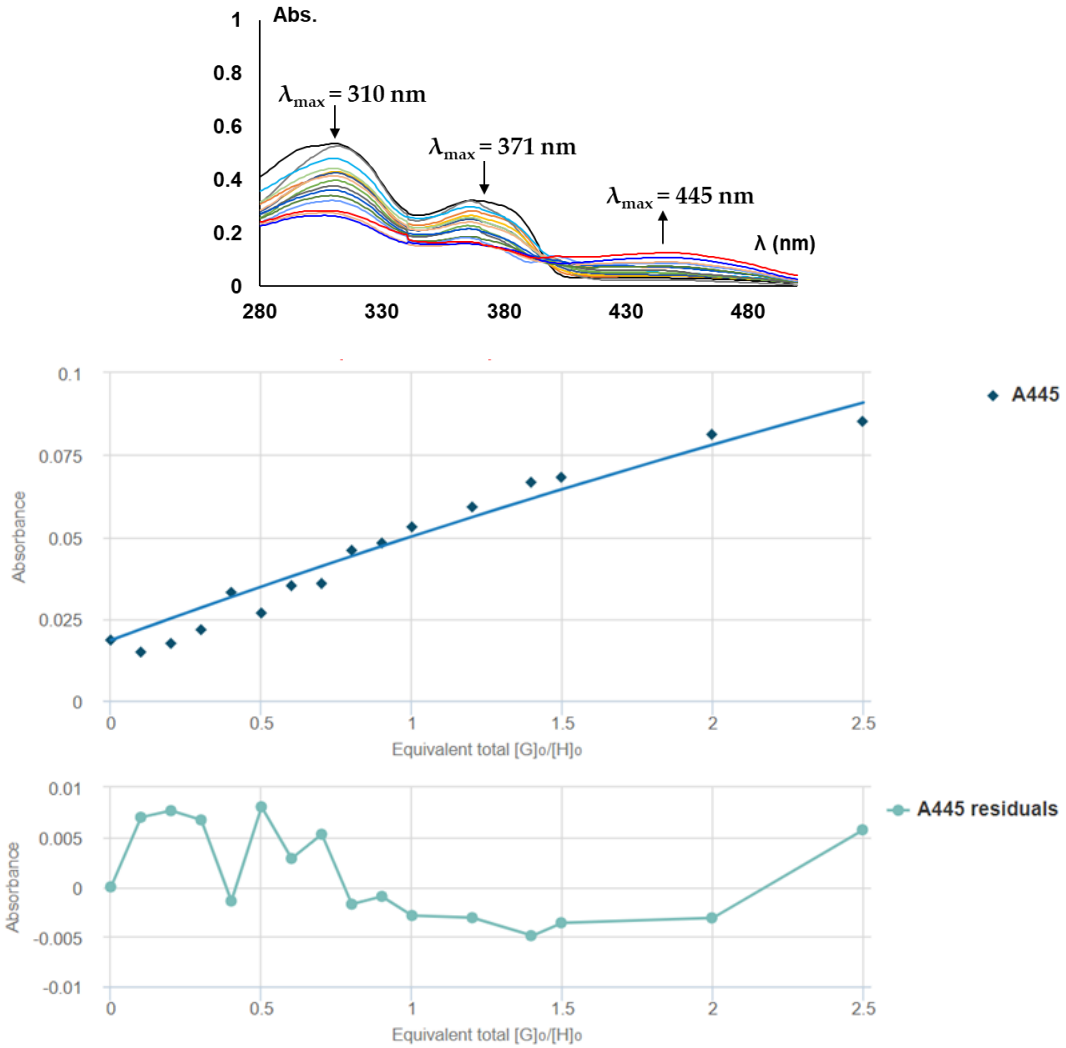


Figure S 18 Fitting the absorbance data from UV-Vis spectra (λ=445 nm) using BindFit (http://app.supramolecular.org/bindfit; stoichiometry 1:1); $K_{11}$=7377.03 error ± 9.8547 %;

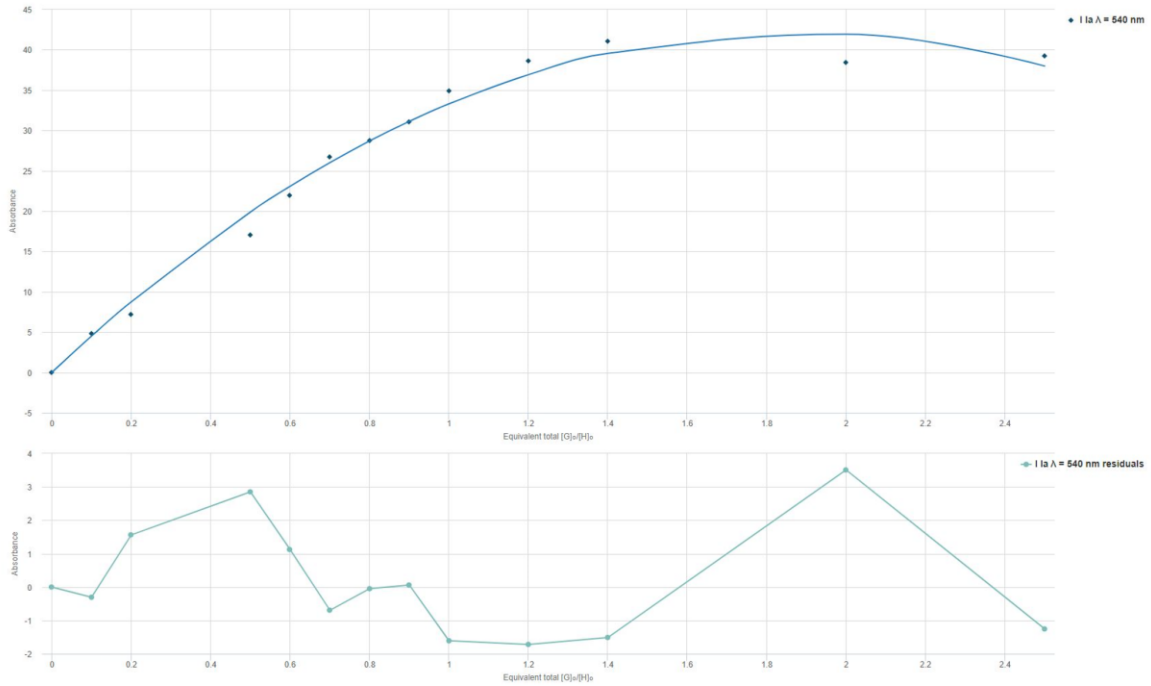


Figure S 19 Fitting fluorescence data (excitation at λ=445 nm) using BindFit (1:**2**)**:** $K_{11}$=77.86 ± 5.96 $M^{-1}$; $K_{12}$=10070.64 ± 845.93 $M^{-1}$

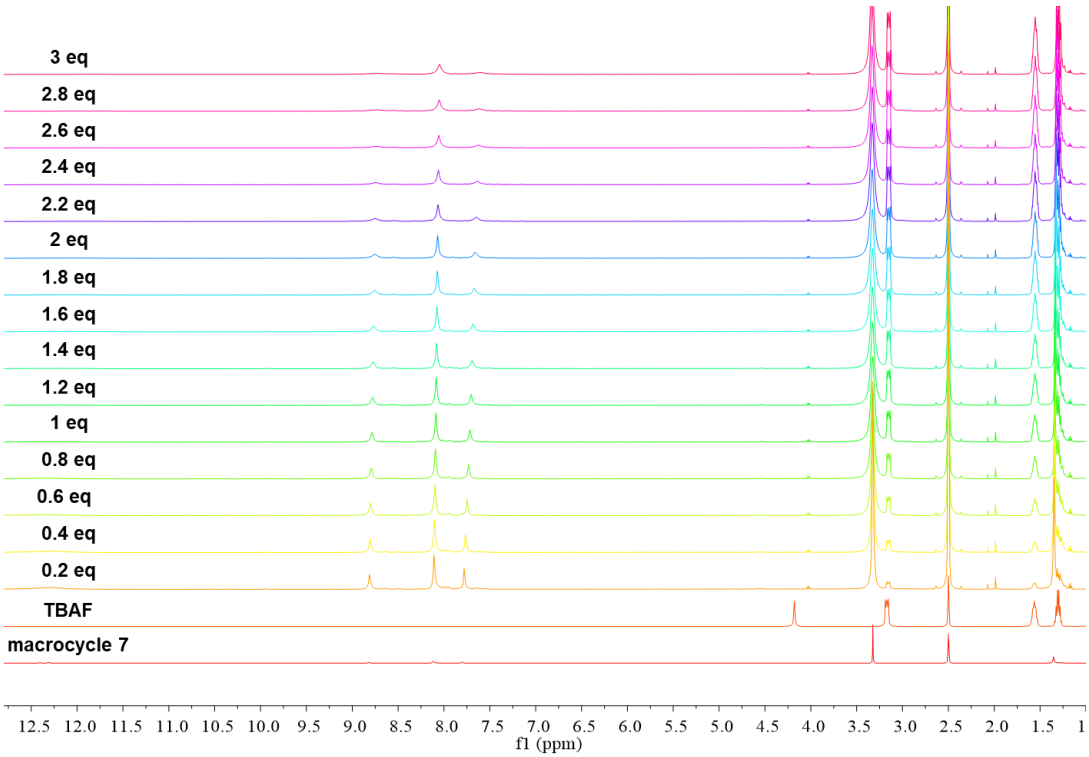


Figure S 20 $^{1}$H NMR spectrum for titration of macrocycle **7** with TBAF (DMSO-*d*$_6$, 500 MHz)

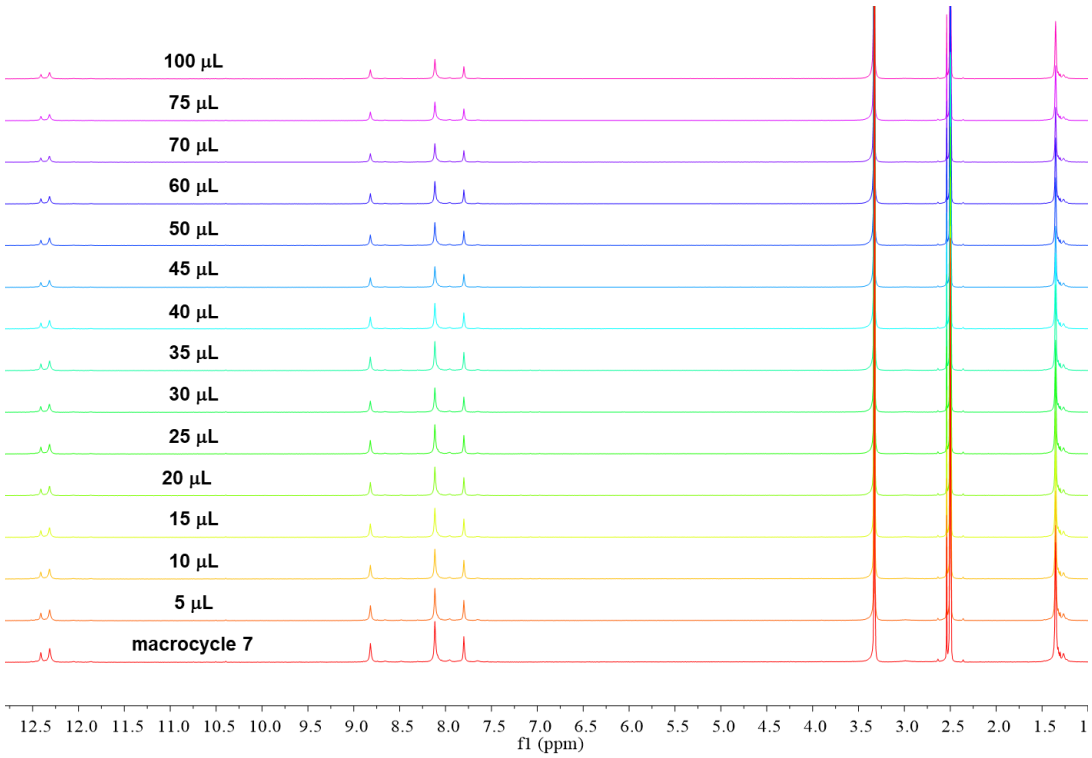


Figure S 21 $^{1}$H NMR spectrum for dilution of macrocycle **7** with DMSO-d$_6$ (DMSO-*d*$_6$, 500 MHz)

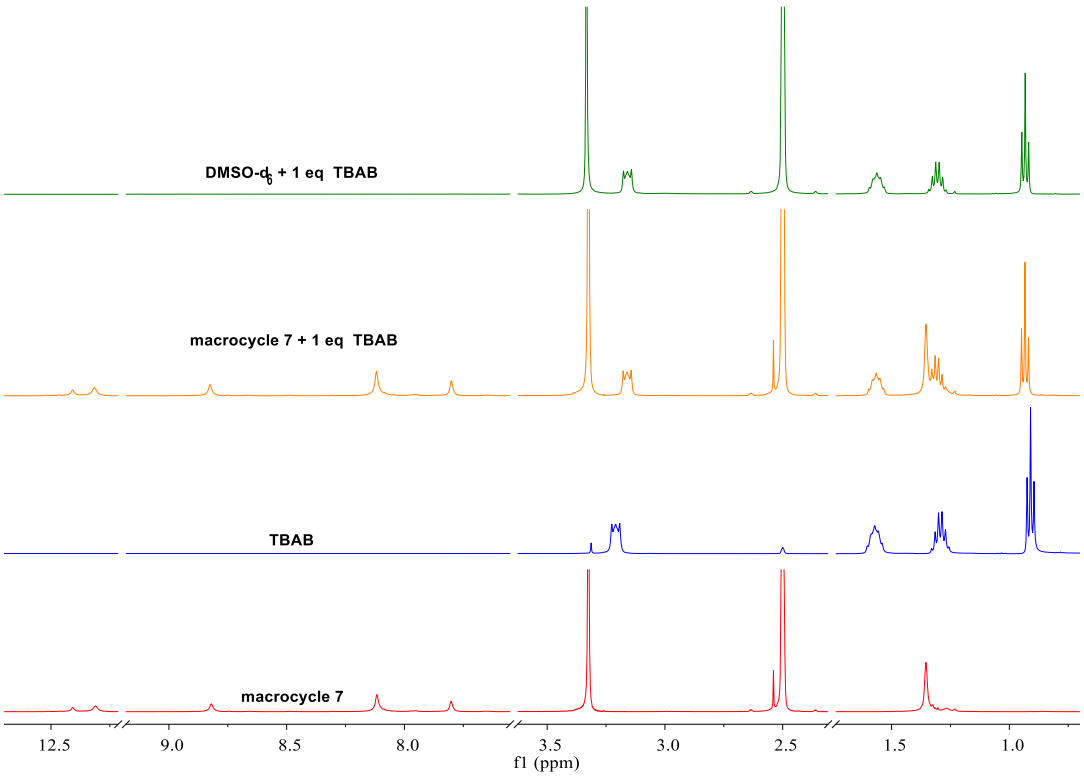


Figure S 22 $^{1}$H NMR spectrum for titration of macrocycle **7** with TBAB (DMSO-$d_6$, 500 MHz)

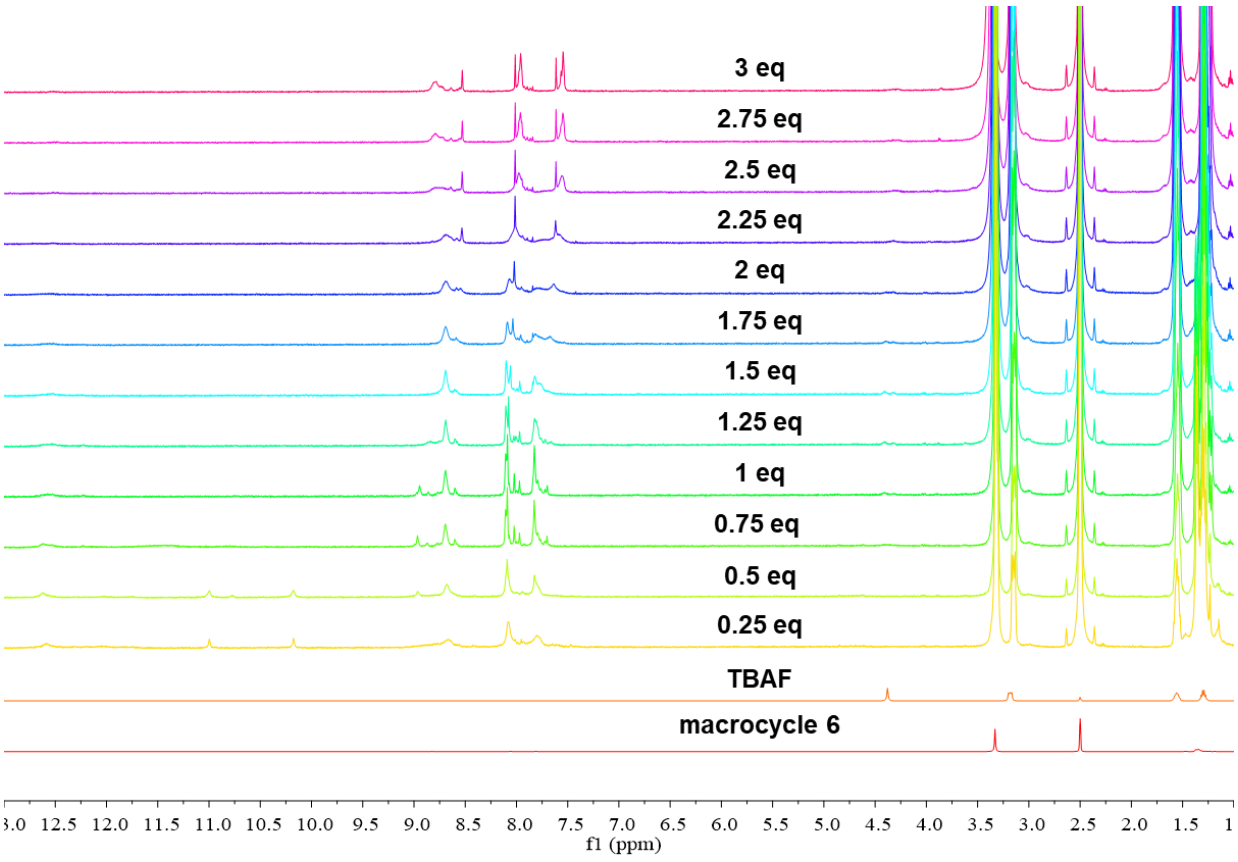


Figure S 23 $^{1}$H NMR spectrum for titration of macrocycle **6** with TBAF (DMSO-$d_6$, 500 MHz)

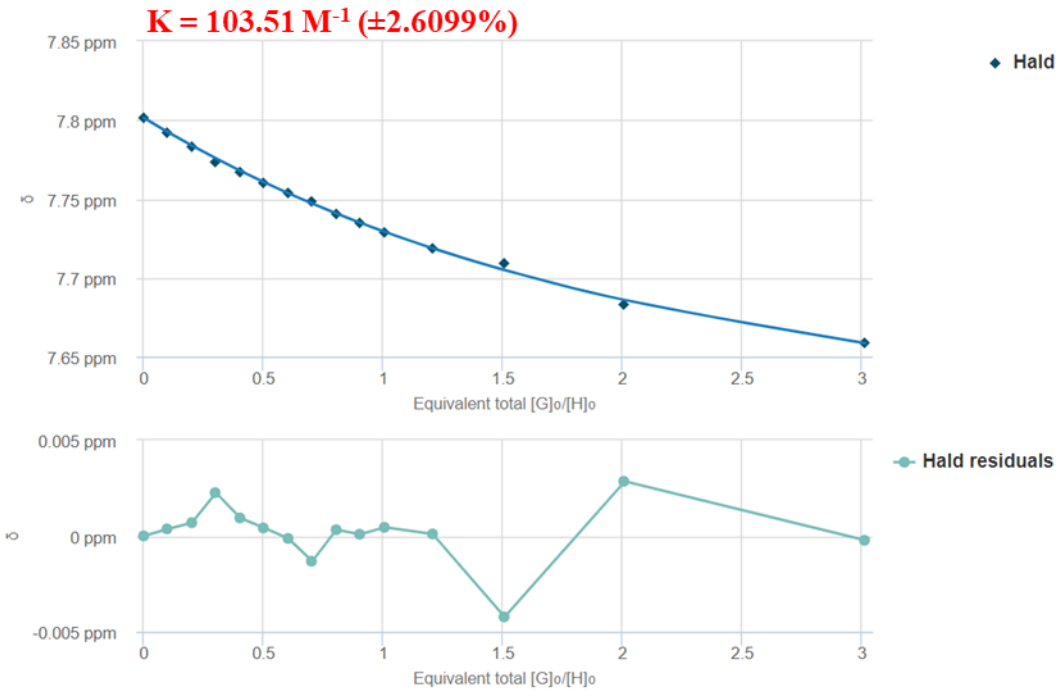


Figure S 24 Fitting NMR data using BindFit (1:1)

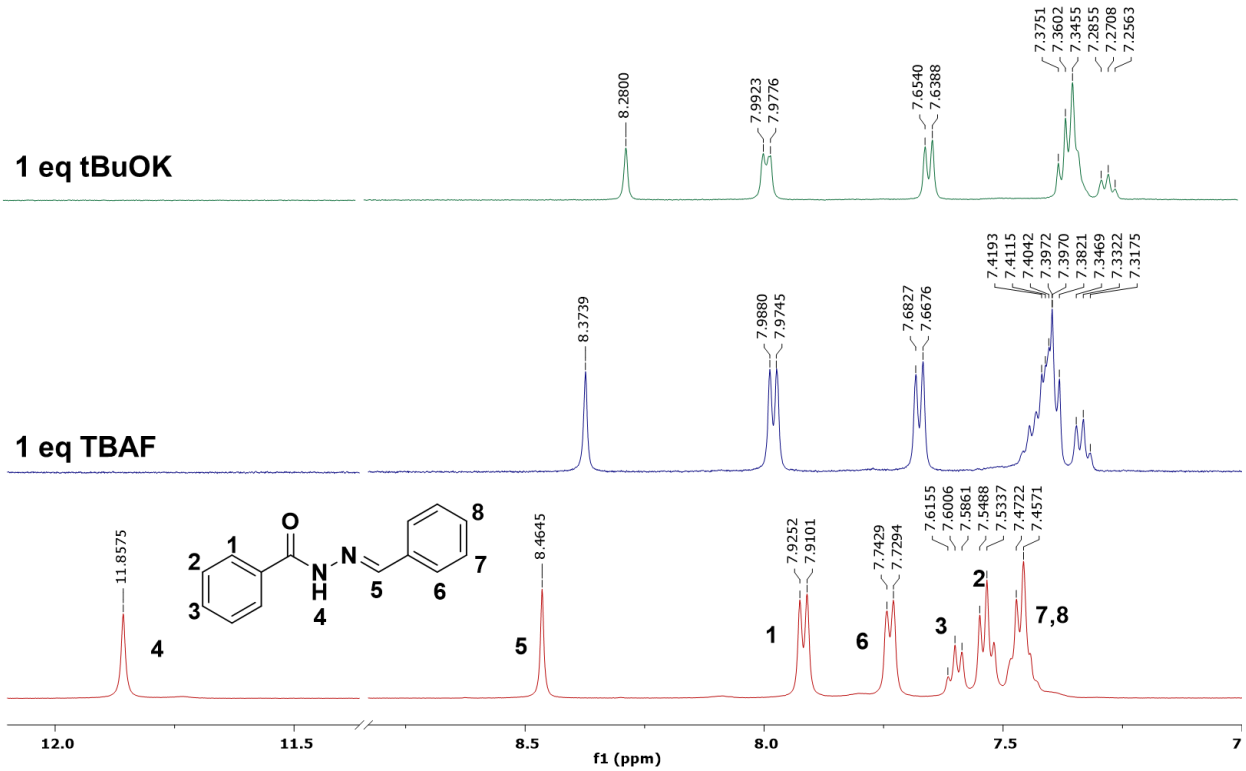


Figure S 25 *N*-acylhydrazone compound in basic medium

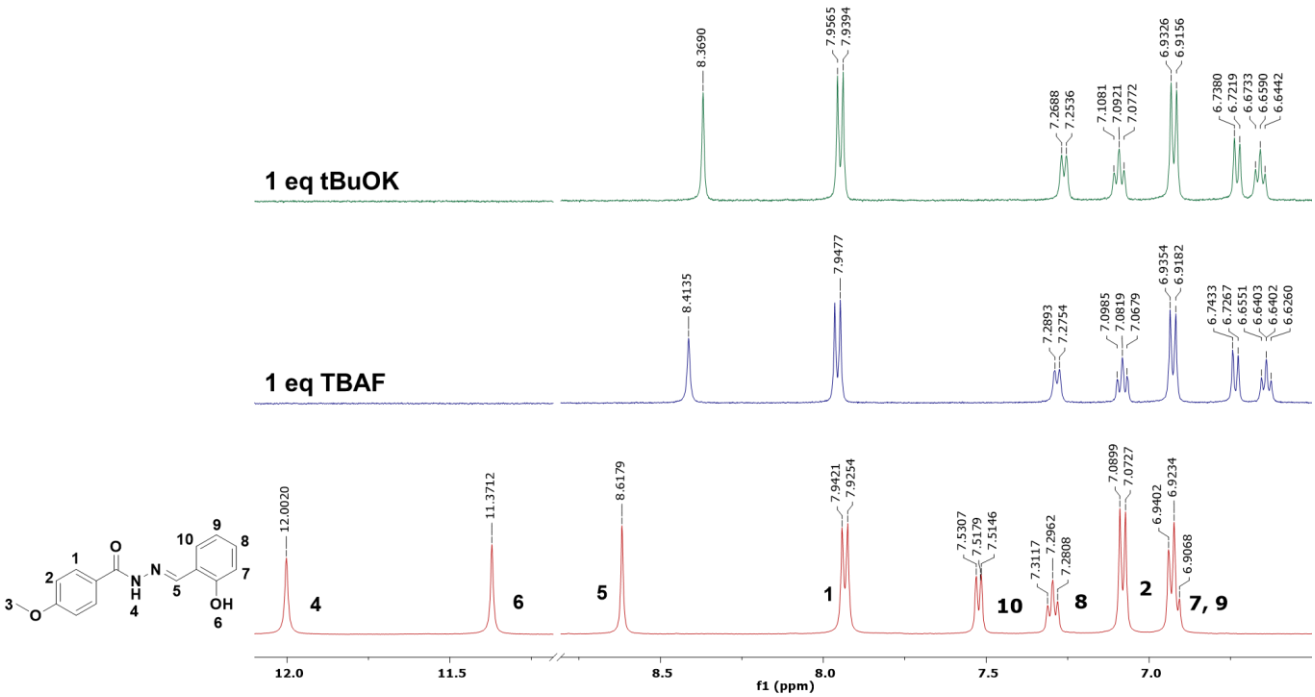


Figure S 26 *N*-acylhydrazone compound with hydroxyl group in basic medium

# 9. HRMS

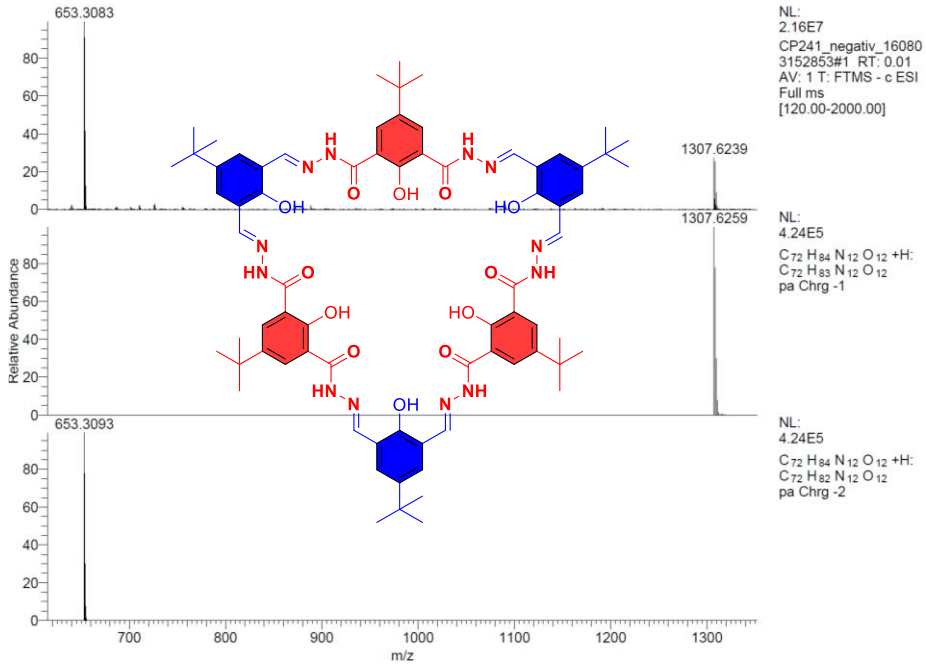


Figure S 27 ESI (-) - HRMS spectrum of compound **6** (top: experimental; bottom: calculated)

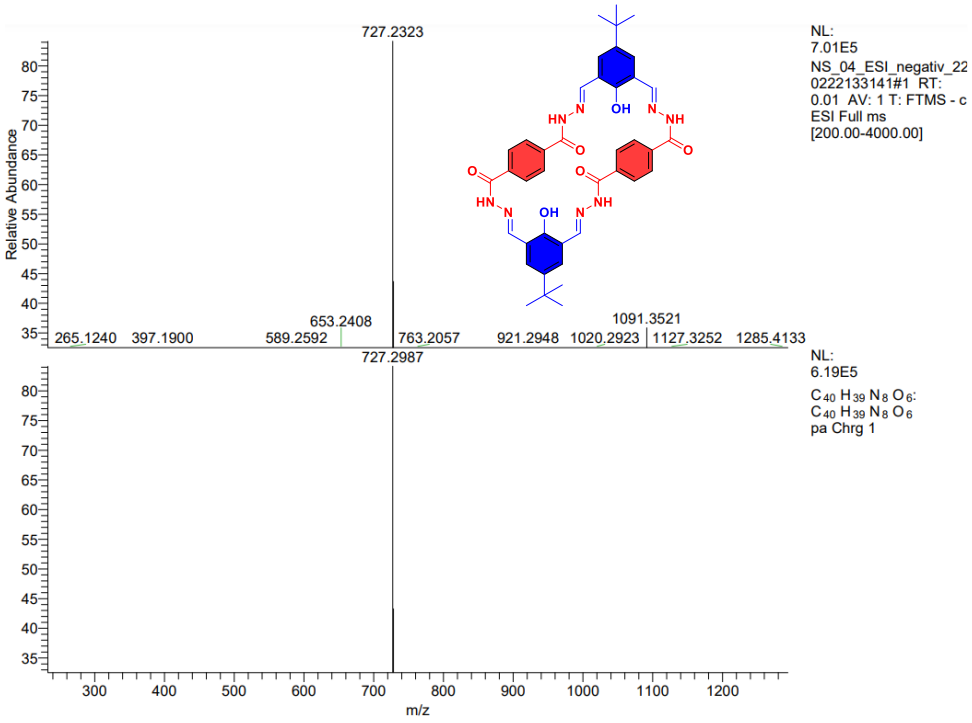


Figure S 28 ESI (-) - HRMS spectrum of compound **7** (top: experimental; bottom: calculated)

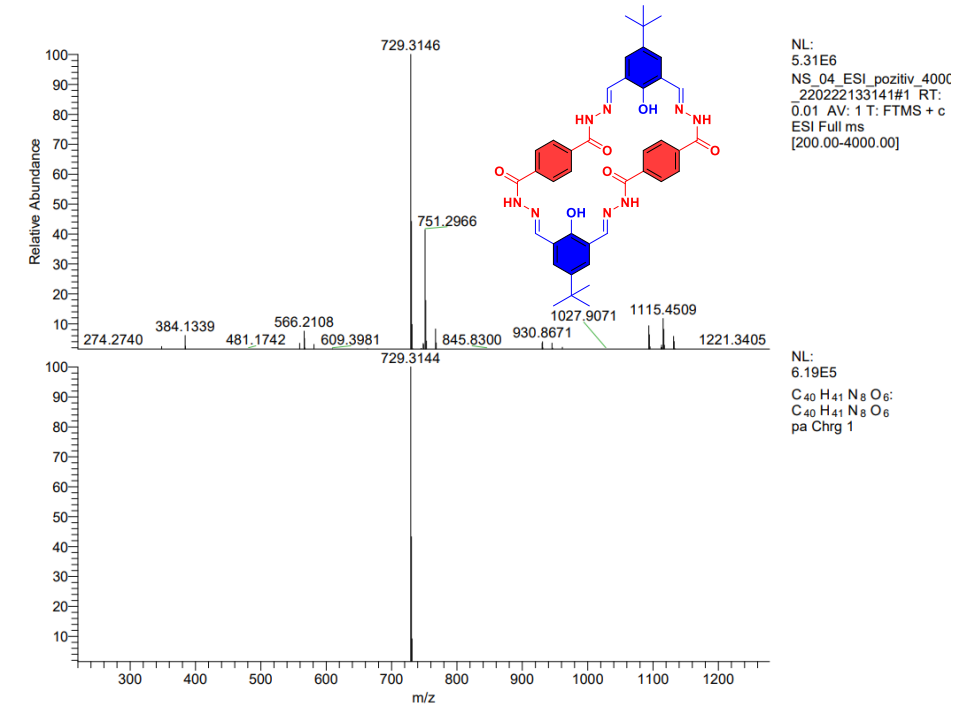


Figure S 29 ESI (+) - HRMS spectrum of compound **7** (top: experimental; bottom: calculated)

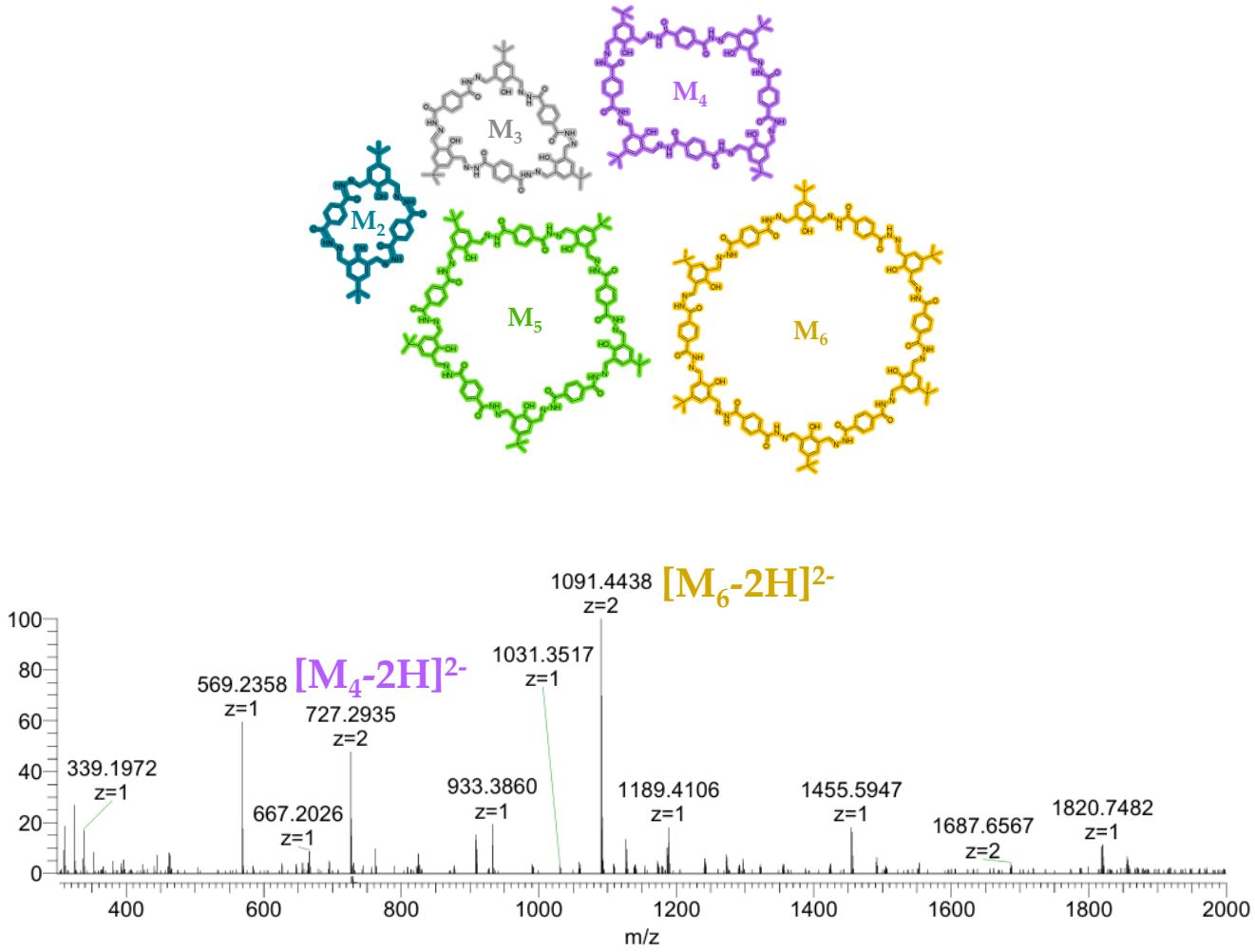


Figure S 30 ESI (+) - HRMS spectrum of compound **7** that was dissolved in DMSO, heated and immediately recorded

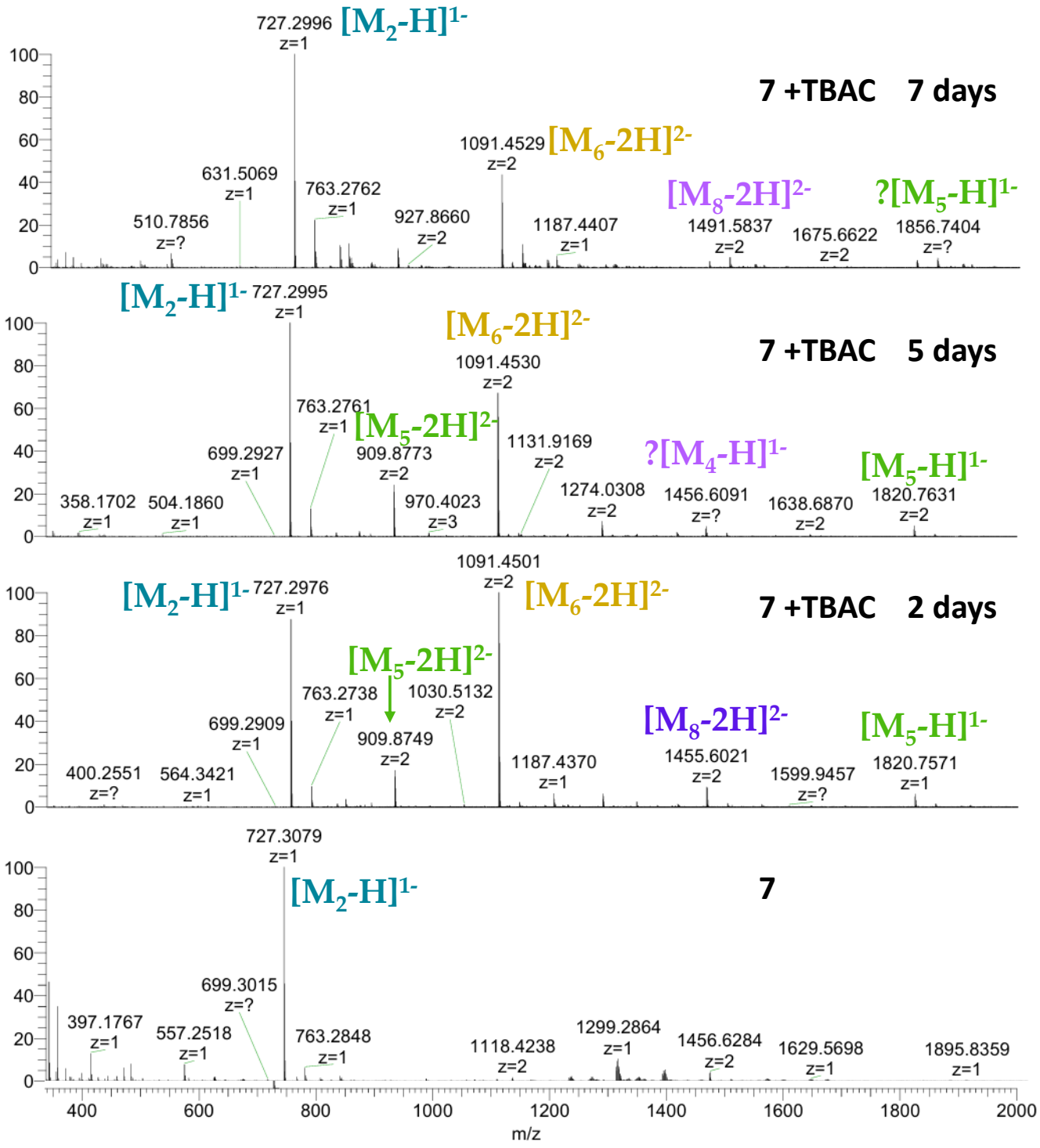


Figure S 31 ESI (+) - HRMS experiments of compound **7** in presence of tetra-*n*-butylammonium chloride (TBAC)

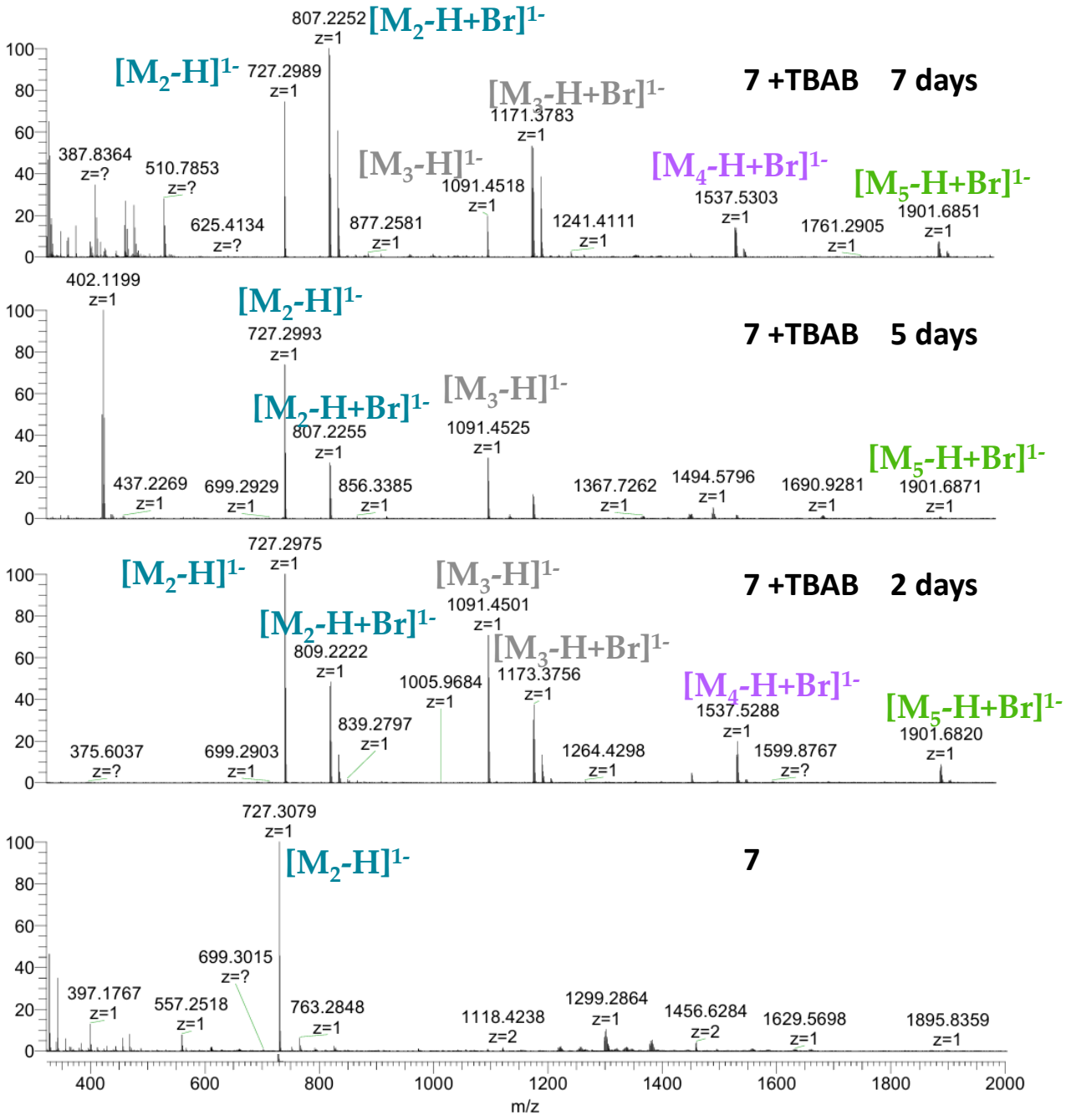


Figure S 32 ESI (+) - HRMS experiments of compound **7** in presence of tetra-*n*-butylammonium bromide (TBAB)

# 10. NMR spectra

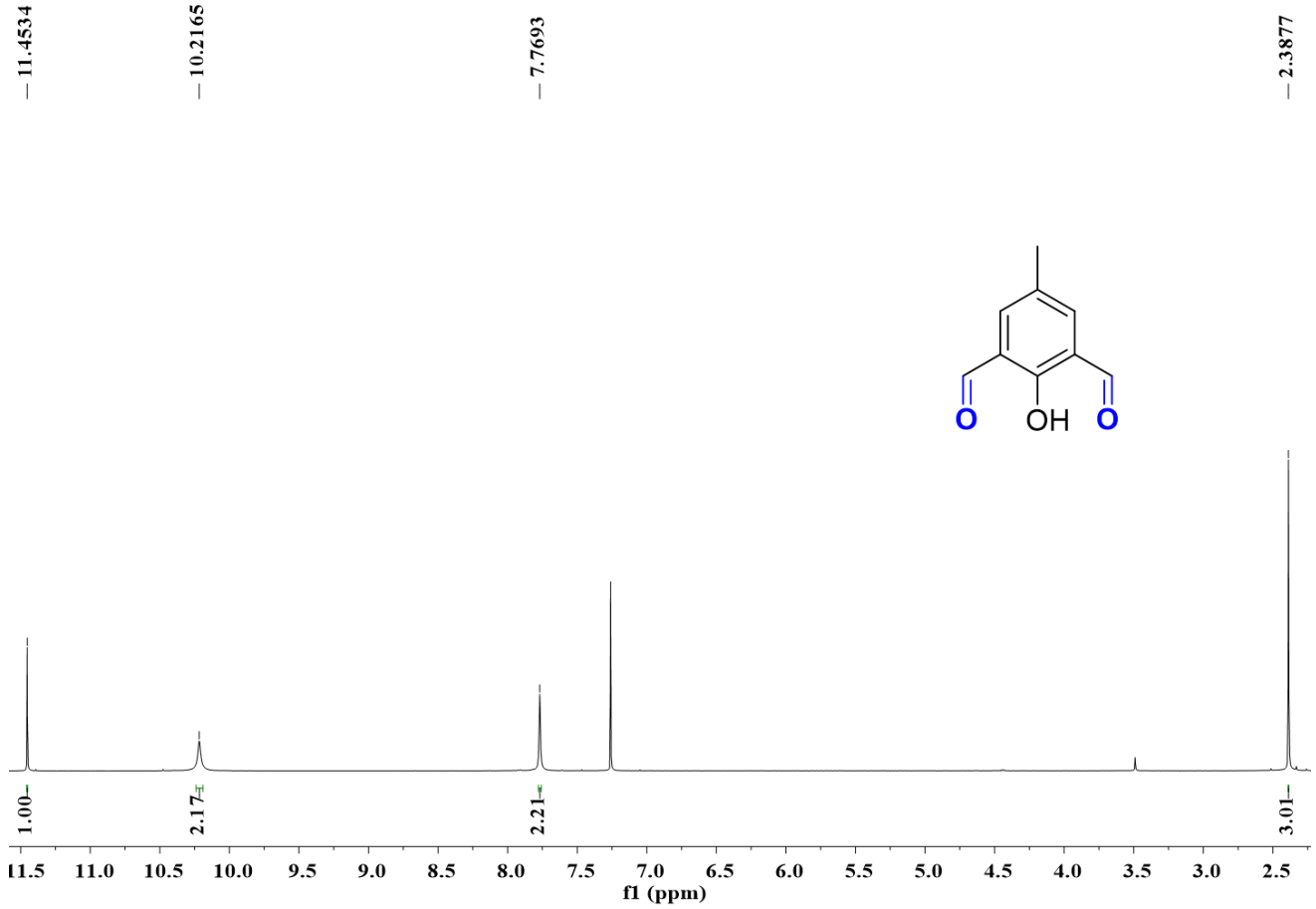


Figure S 33 $^{1}$H NMR spectrum of compound **1a** ($CDCl_3$, 500 MHz)

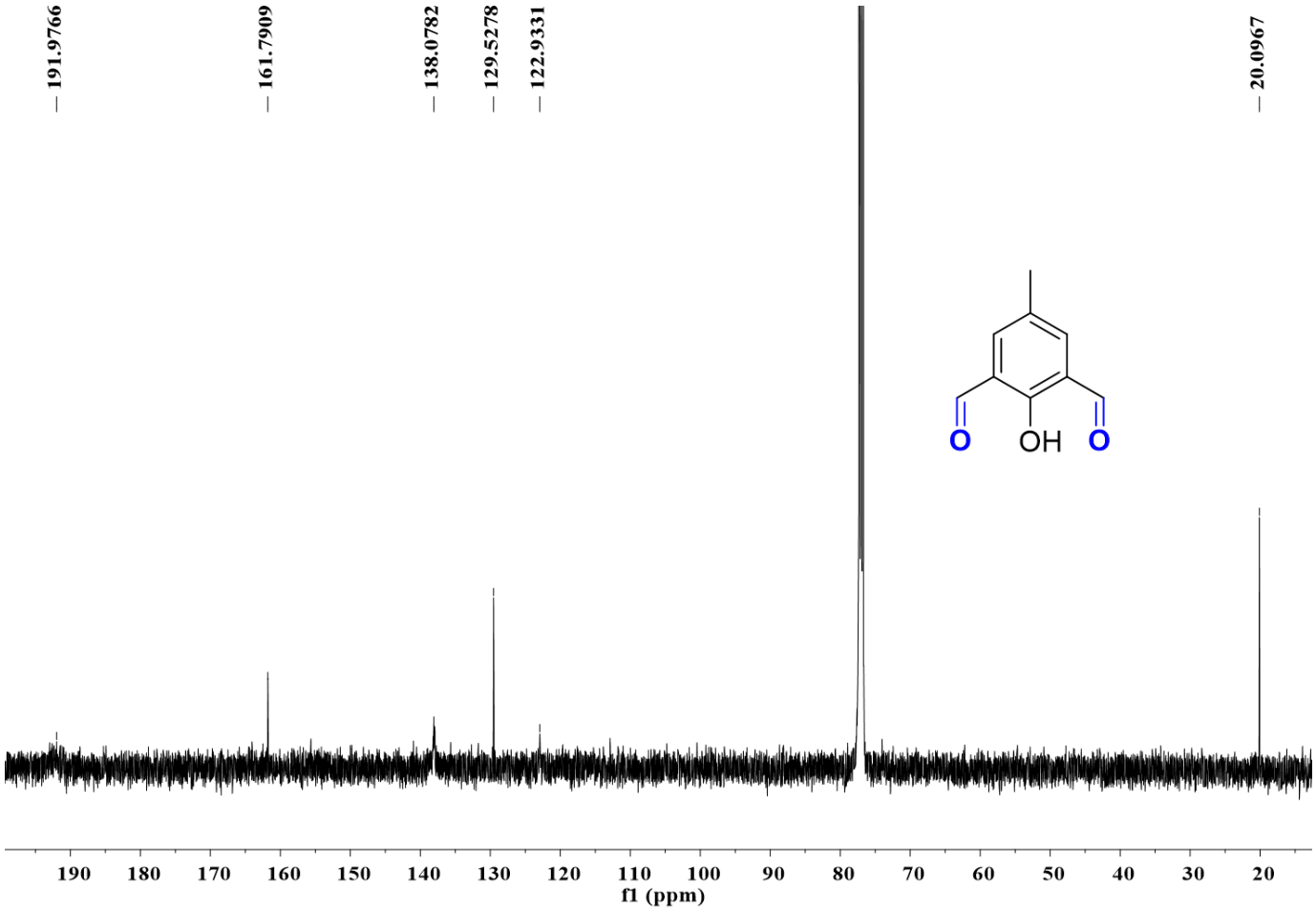


Figure S 34 $^{13}C$ NMR spectrum of compound **1a** ($CDCl_3$, 125 MHz)

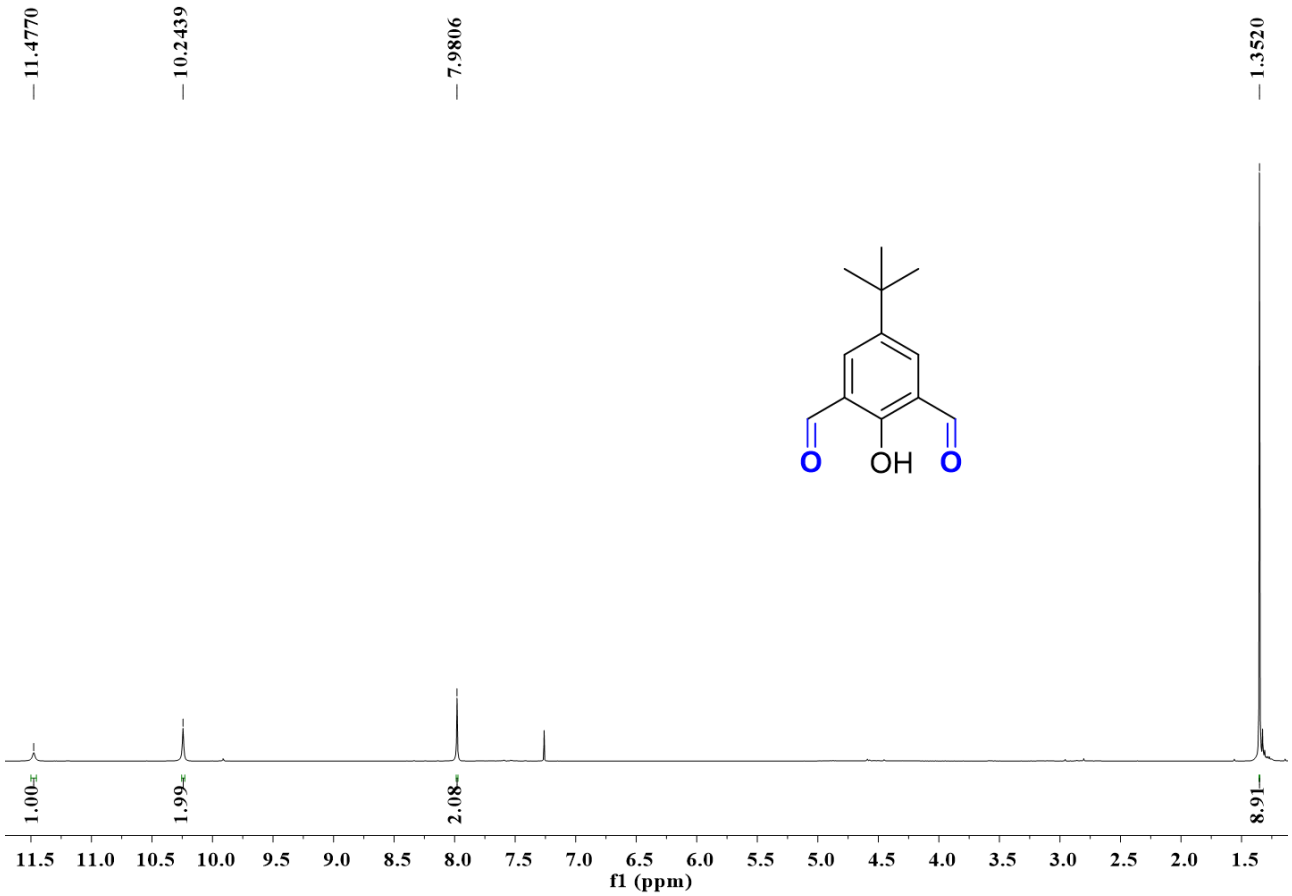


Figure S 35 $^{1}$H NMR spectrum of compound **1b** ($CDCl_3$, 500 MHz)

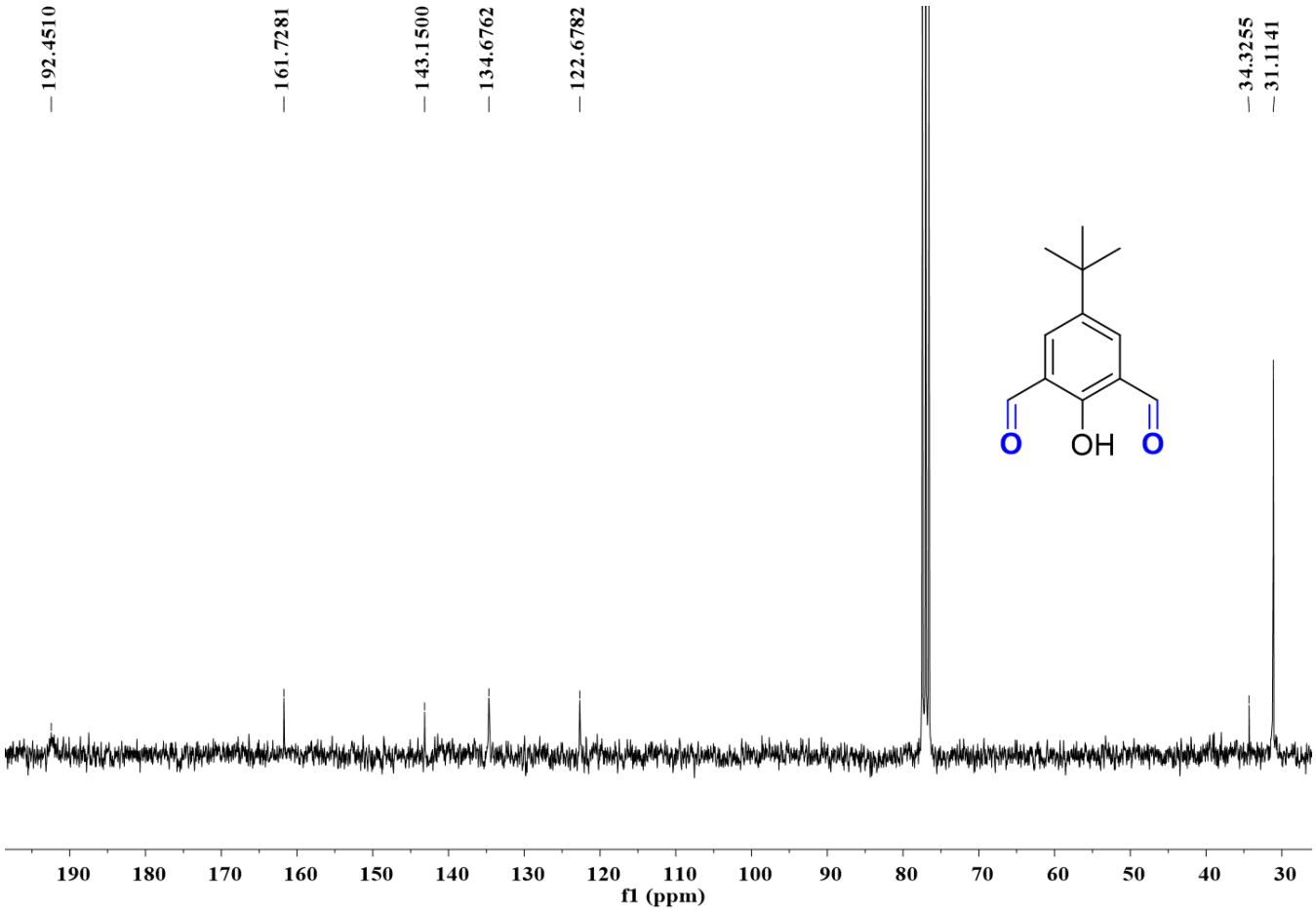


Figure S 36 $^{13}C$ NMR spectrum of compound **1b** ($CDCl_3$,125 MHz

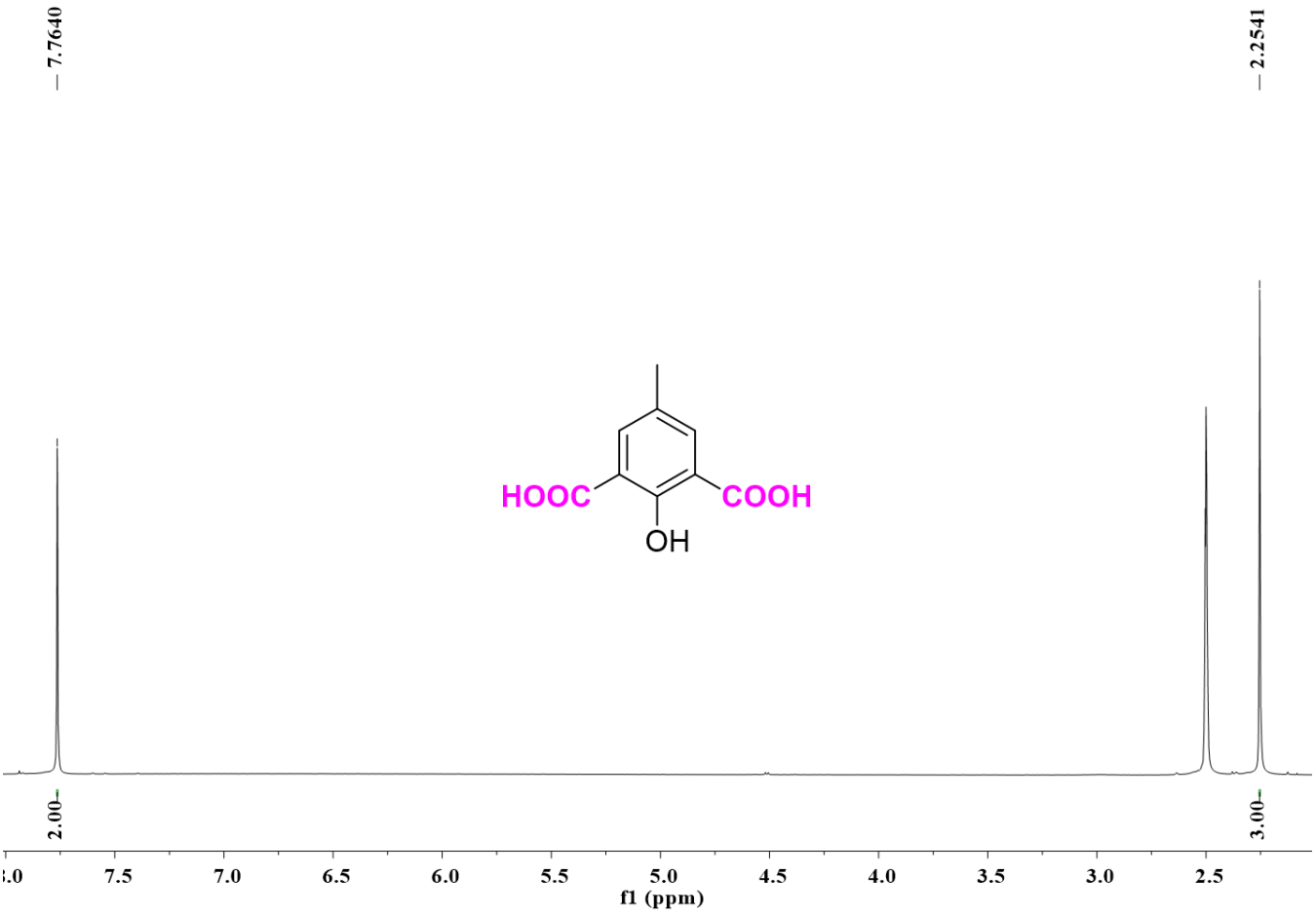


Figure S 37 $^{1}$H NMR spectrum of compound **4a** (DMSO-$d_6$, 500 MHz)

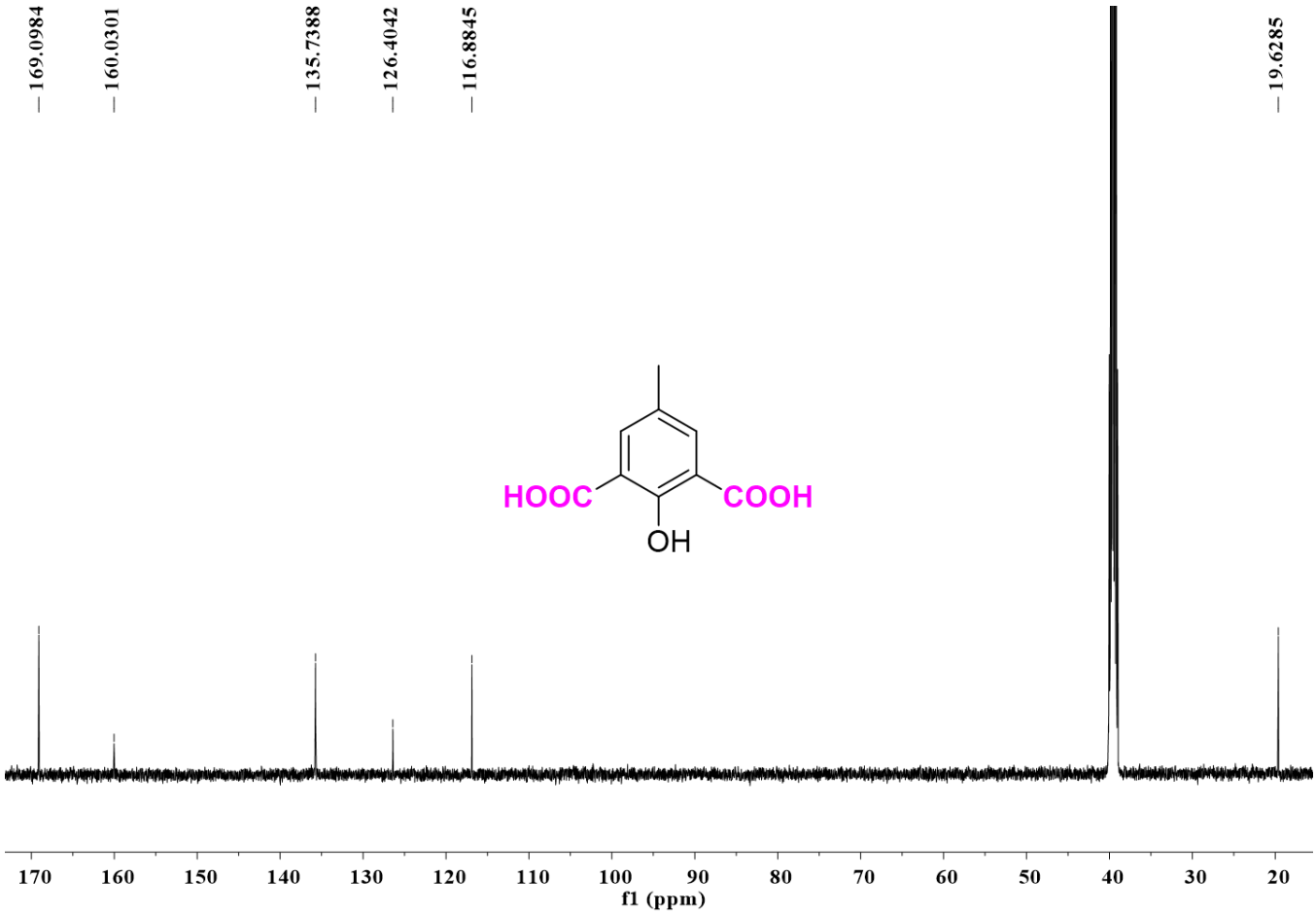


Figure S 38 $^{13}C$ NMR spectrum of compound **4a** (DMSO-$d_6$, 125 MHz)

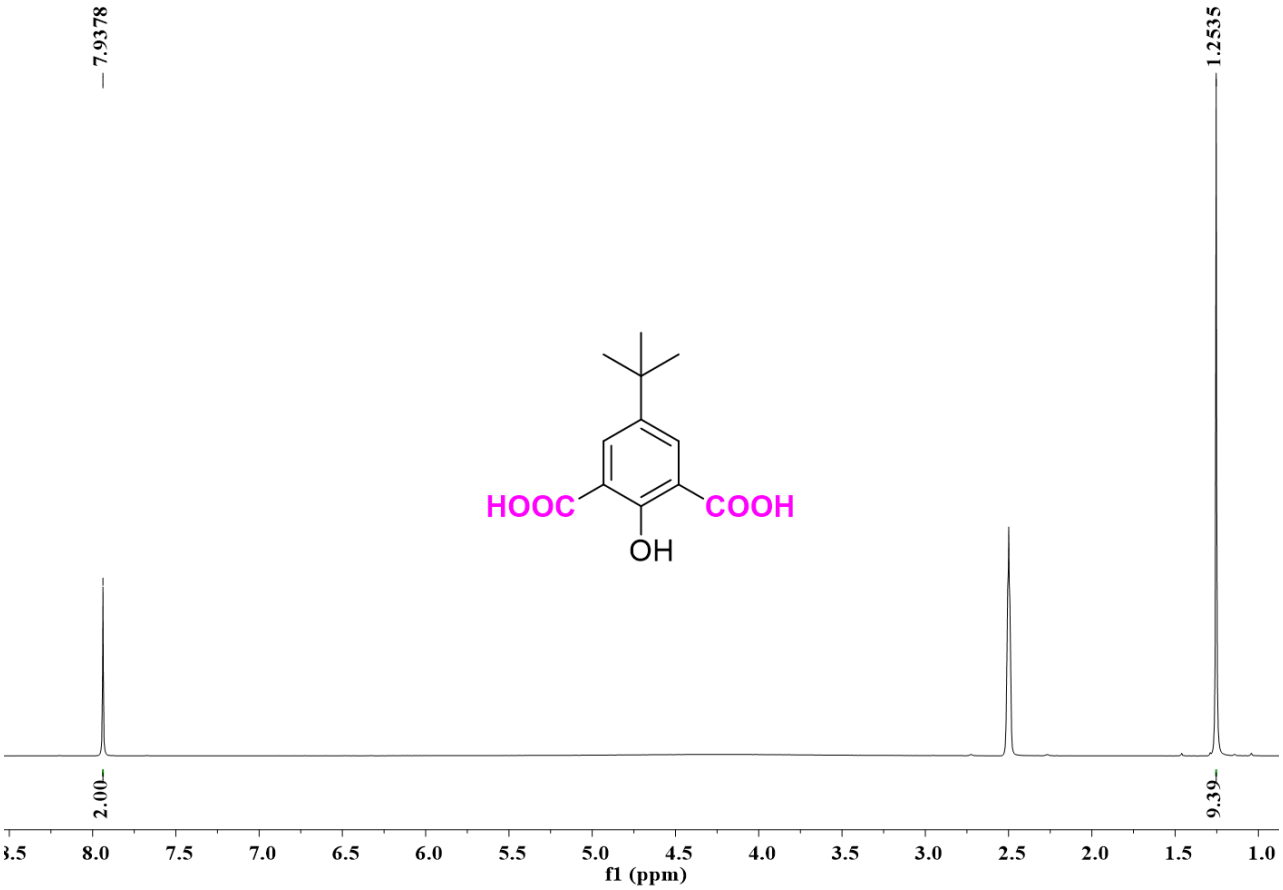


Figure S 39 $^{1}$H NMR spectrum of compound **4b** (DMSO-$d_6$, 500 MHz)

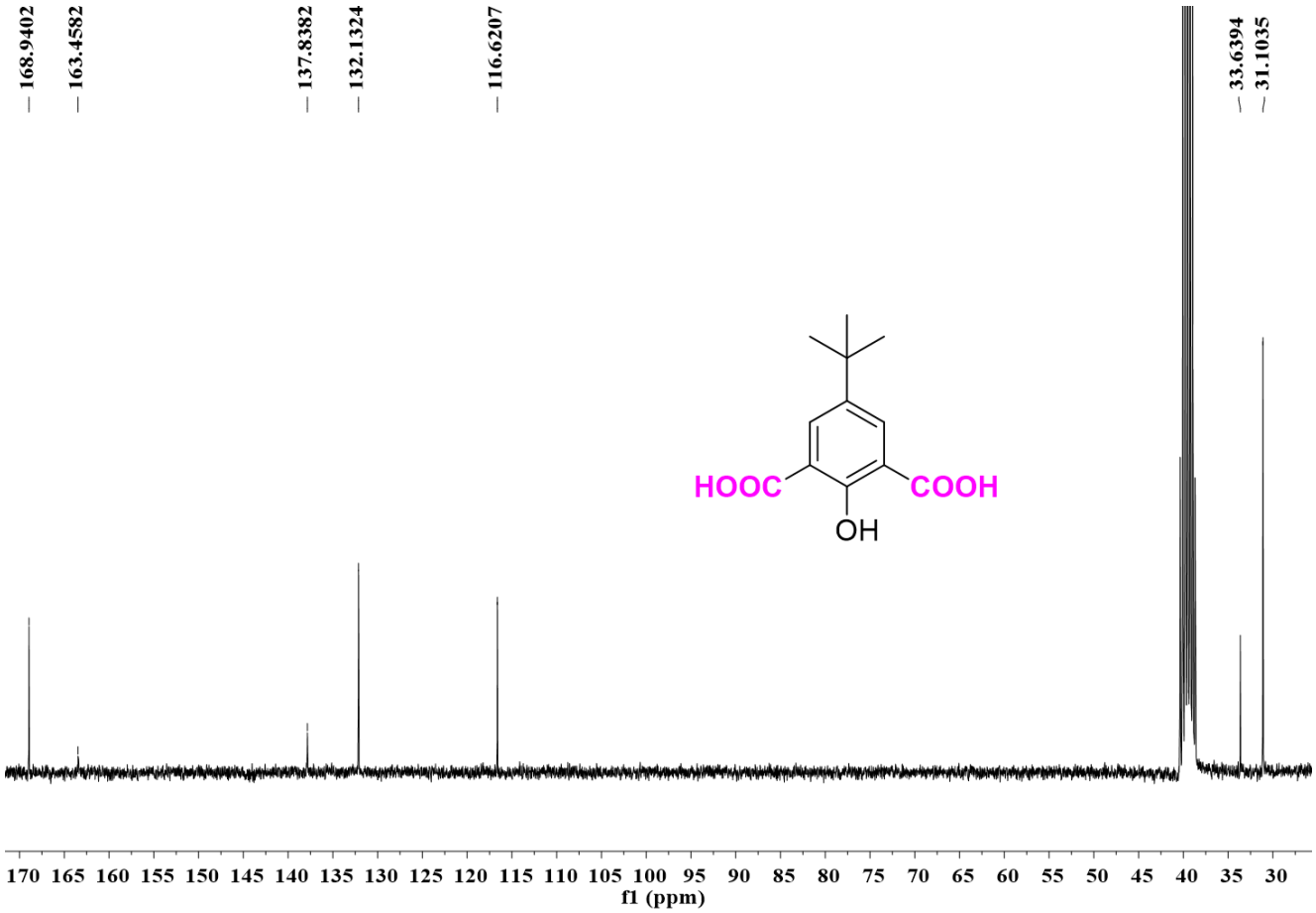


Figure S 40 $^{13}C$ NMR spectrum of compound **4b** (DMSO-$d_6$, 125 MHz)

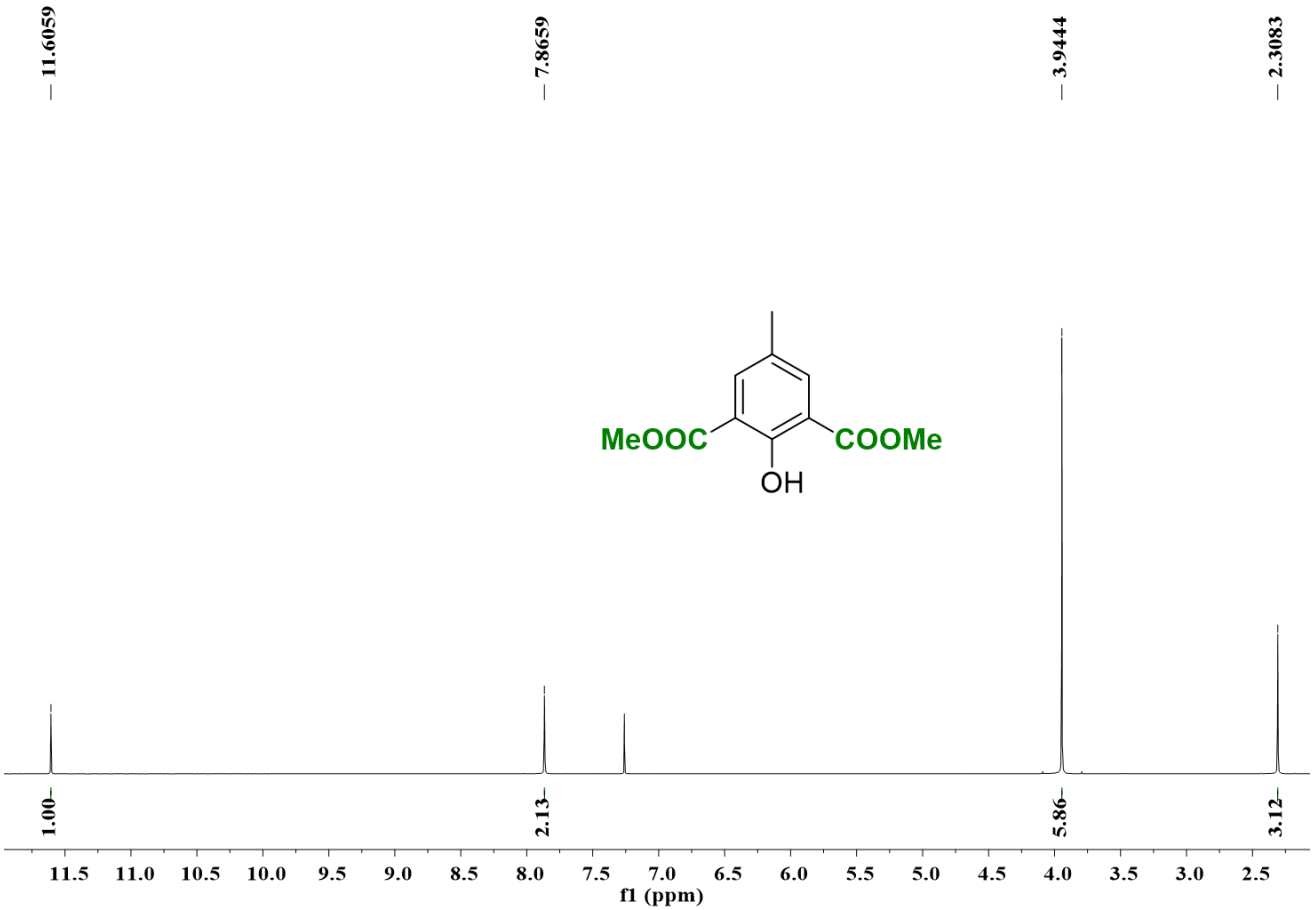


Figure S 41 $^{1}$H NMR spectrum of compound **5a** (DMSO-$d_6$, 500 MHz)

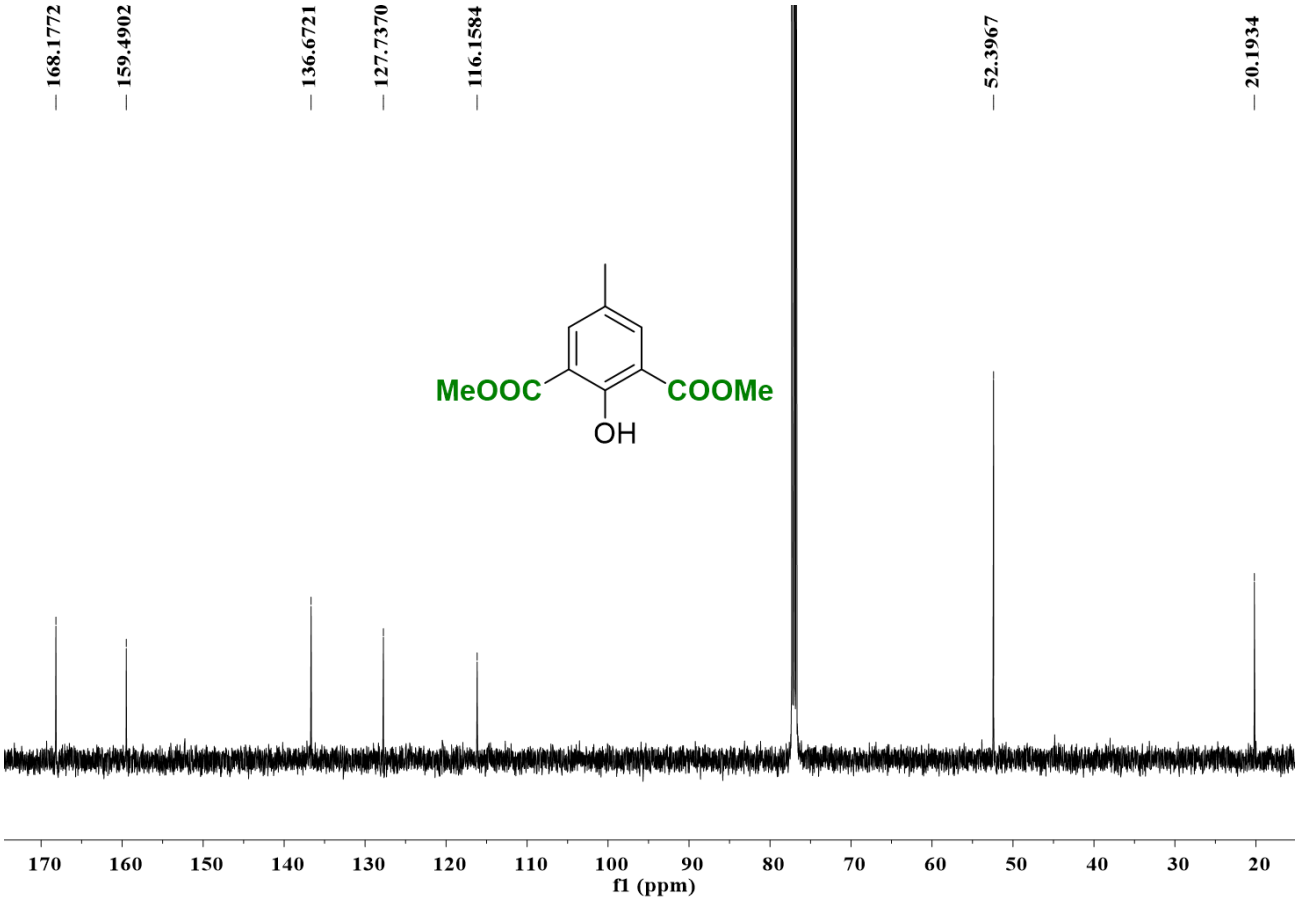


Figure S 42 $^{13}$C NMR spectrum of compound **5a** (DMSO-$d_6$, 125 MHz)

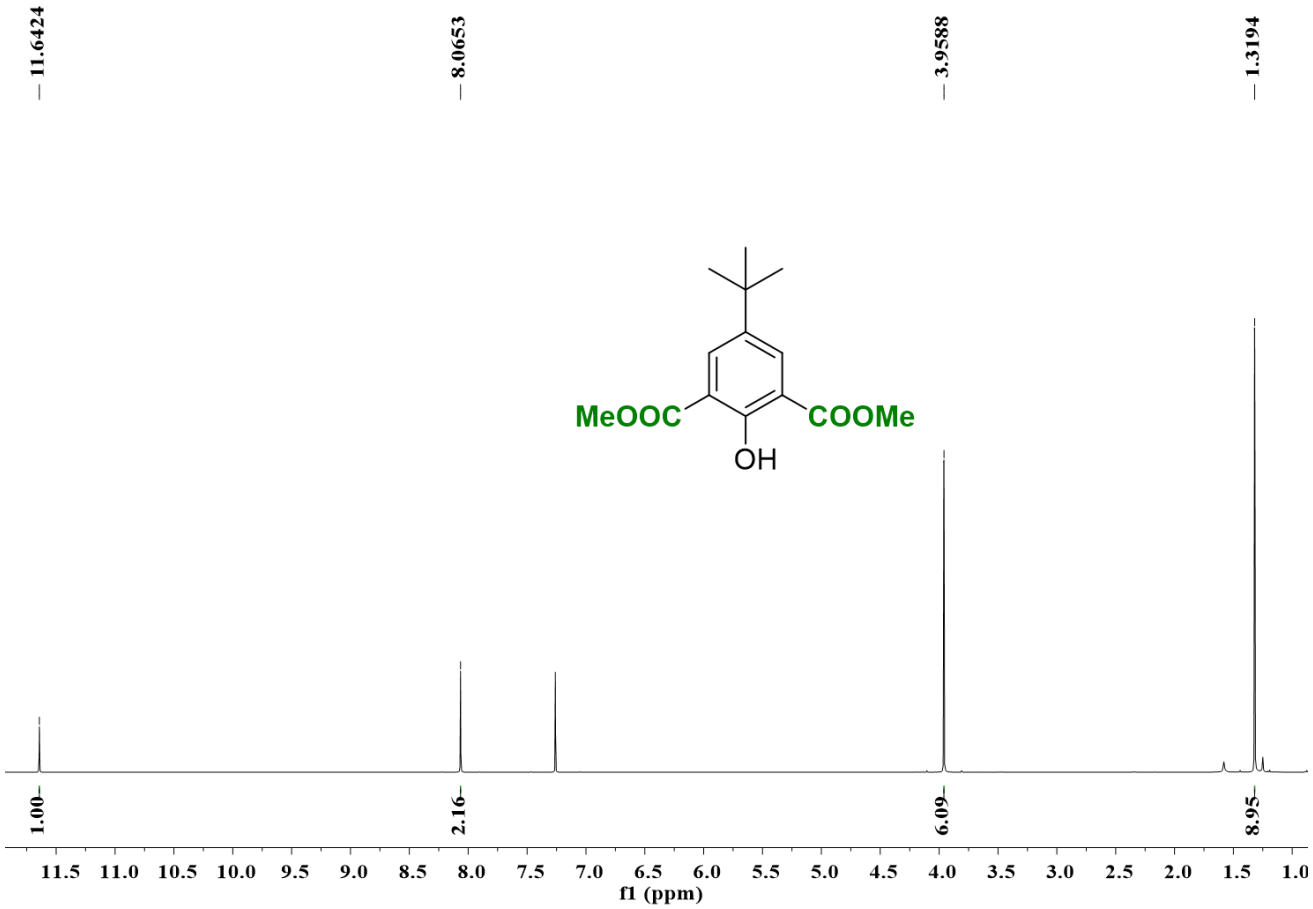


Figure S 43 $^{1}$H NMR spectrum of compound **5b** (DMSO-$d_6$, 500 MHz)

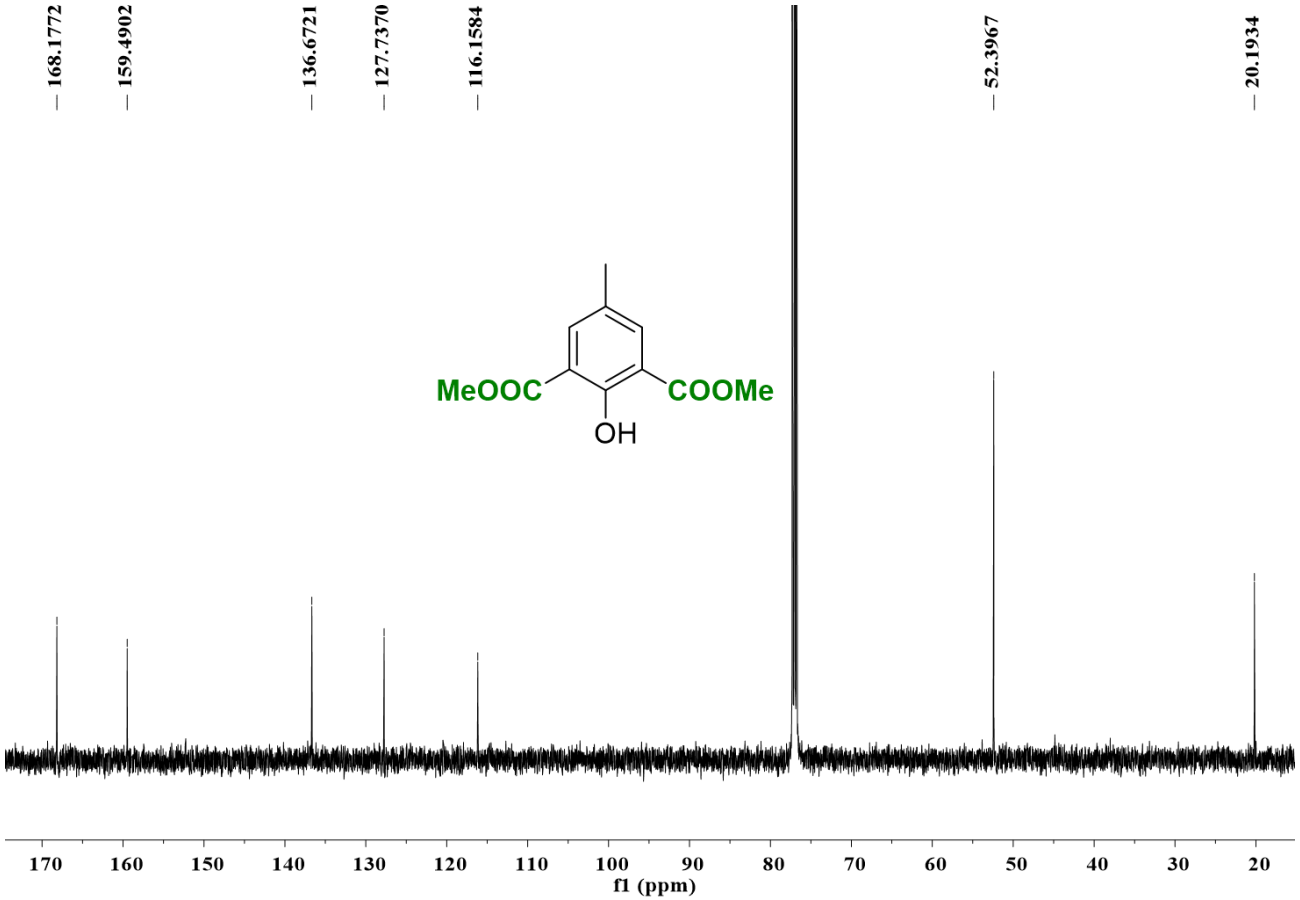


Figure S 44 $^{13}C$ NMR spectrum of compound **5b** (DMSO-$d_6$, 125 MHz)

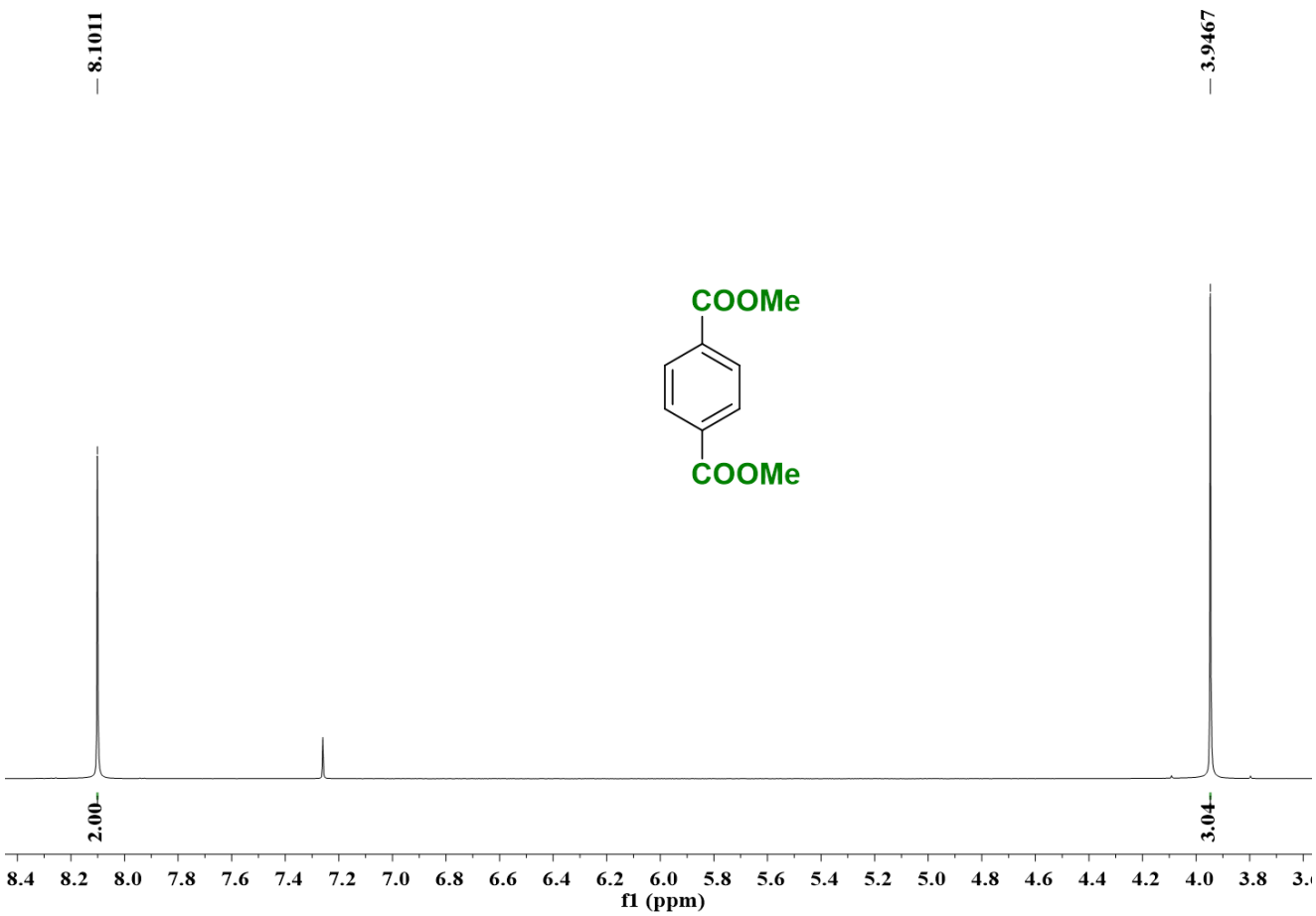


Figure S 45 $^{1}$H NMR spectrum of compound **8** (DMSO-$d_6$, 500 MHz)

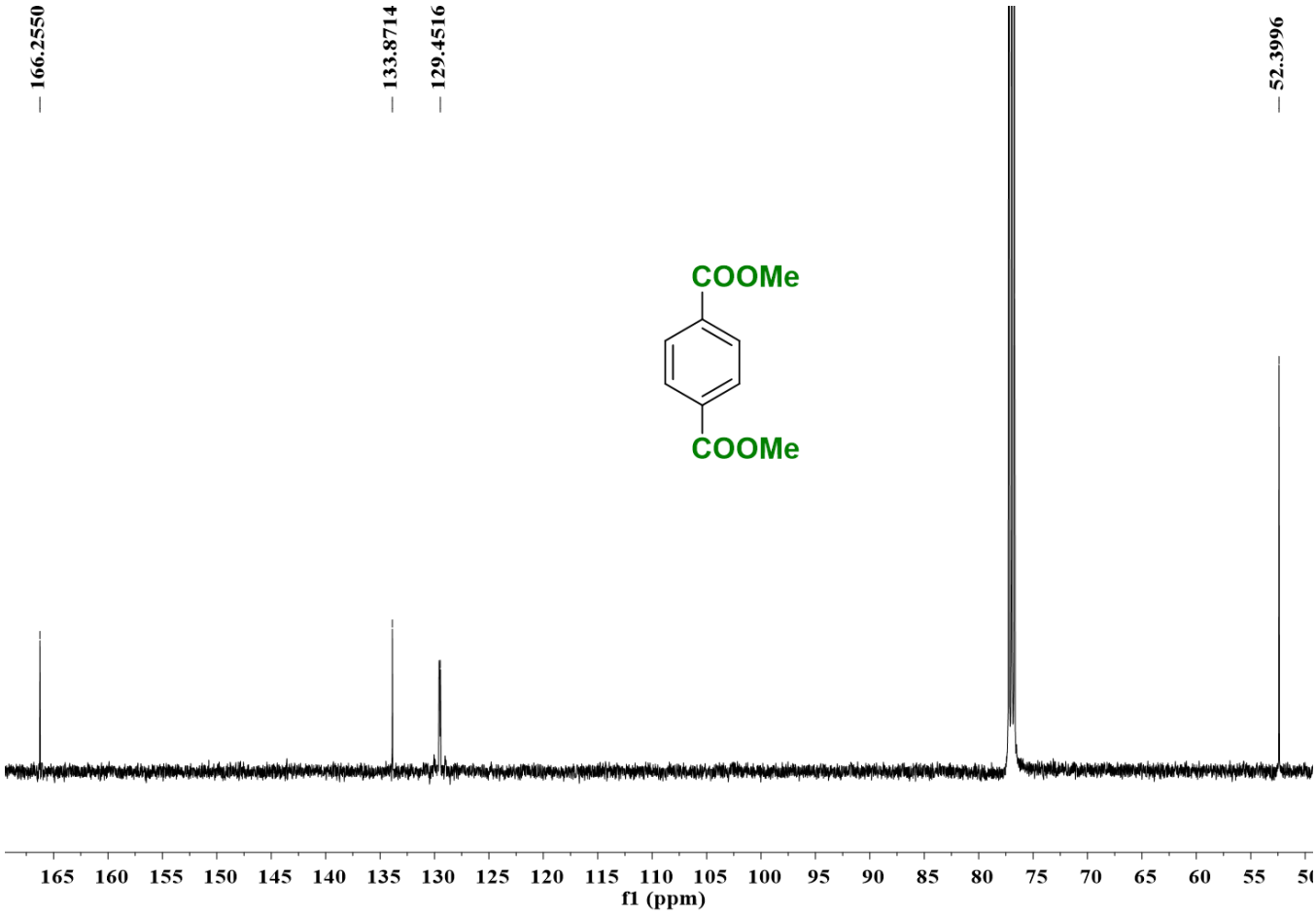


Figure S 46 $^{13}$C NMR spectrum of compound **8** (DMSO-$d_6$, 125 MHz)

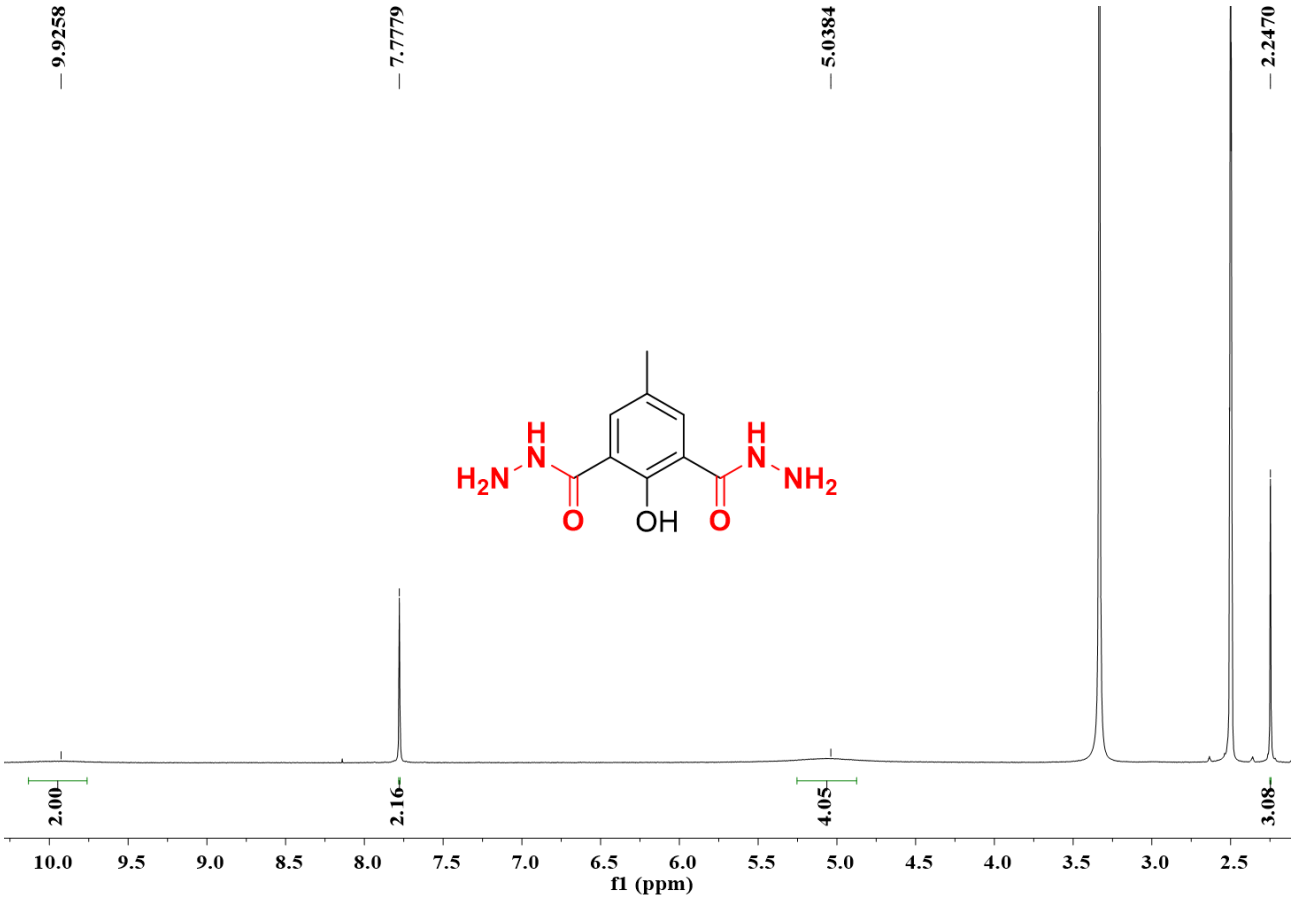


Figure S 47 $^{1}$H NMR spectrum of compound **2a** (DMSO-$d_6$, 500 MHz)

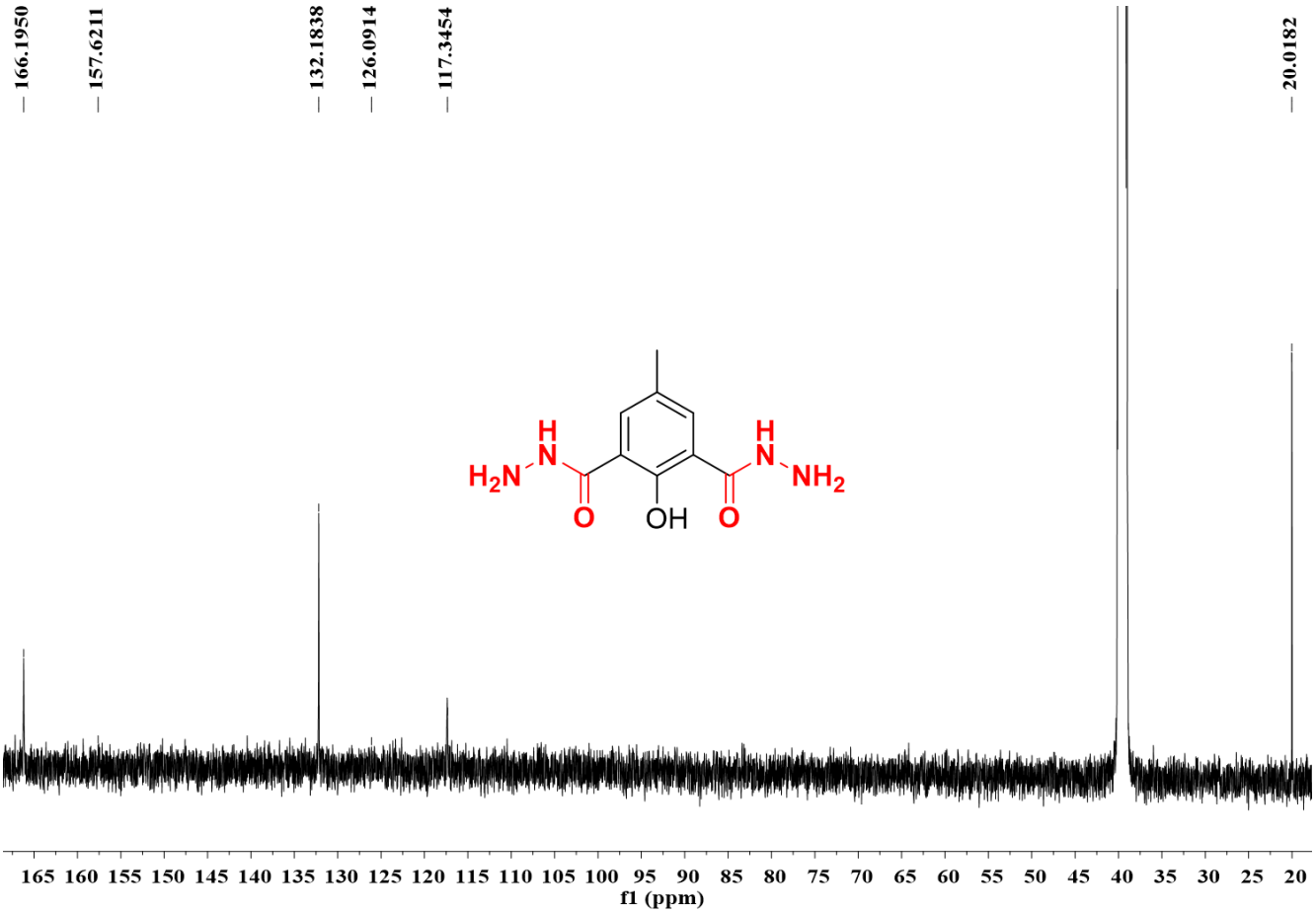


Figure S 48 $^{13}C$ NMR spectrum of compound **2a** (DMSO-$d_6$, 125 MHz)

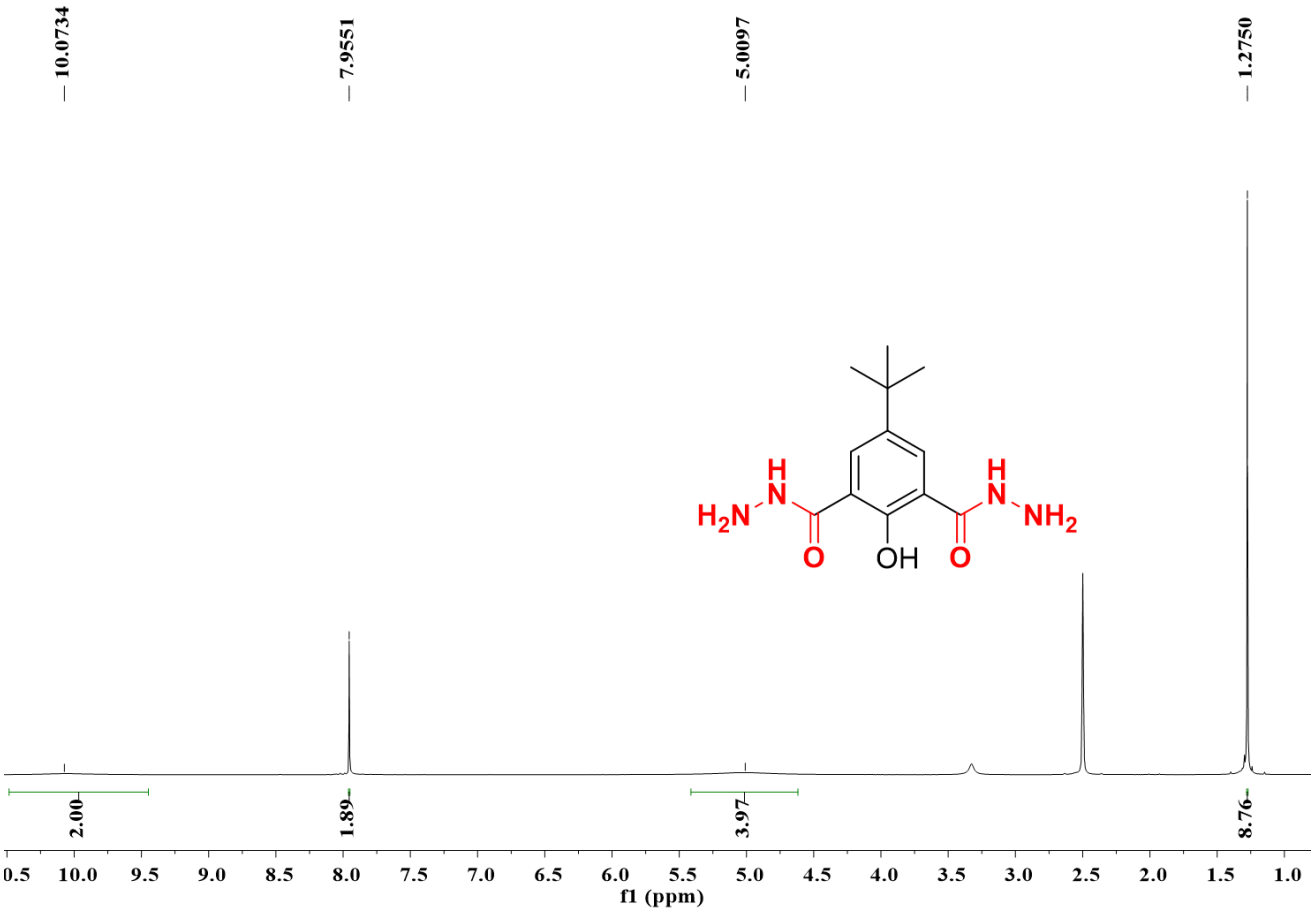


Figure S 49 $^{1}$H NMR spectrum of compound **2b** (DMSO-$d_6$, 500 MHz)

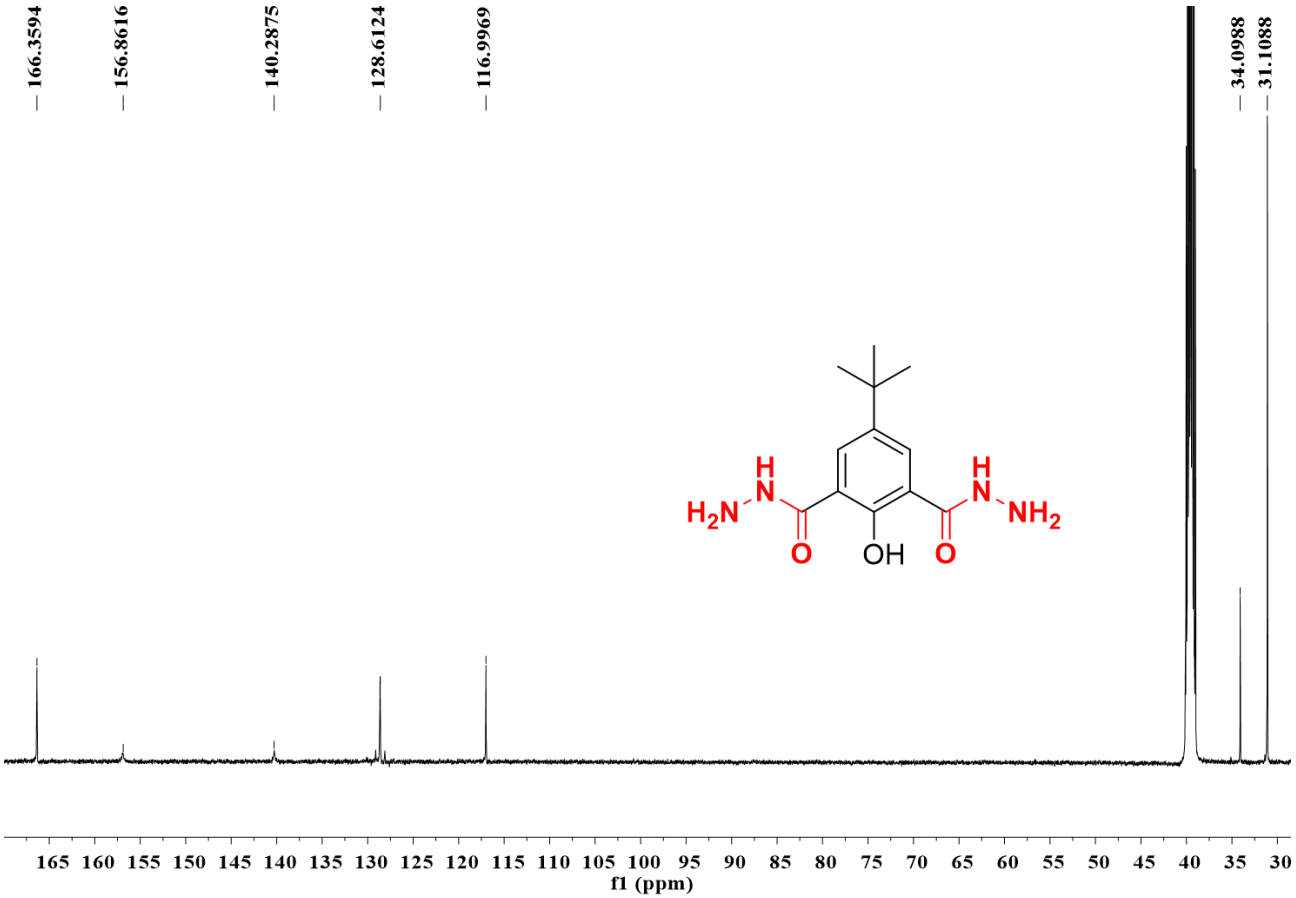


Figure S 50 $^{13}$C NMR spectrum of compound **2b** (DMSO-$d_6$, 125 MHz)

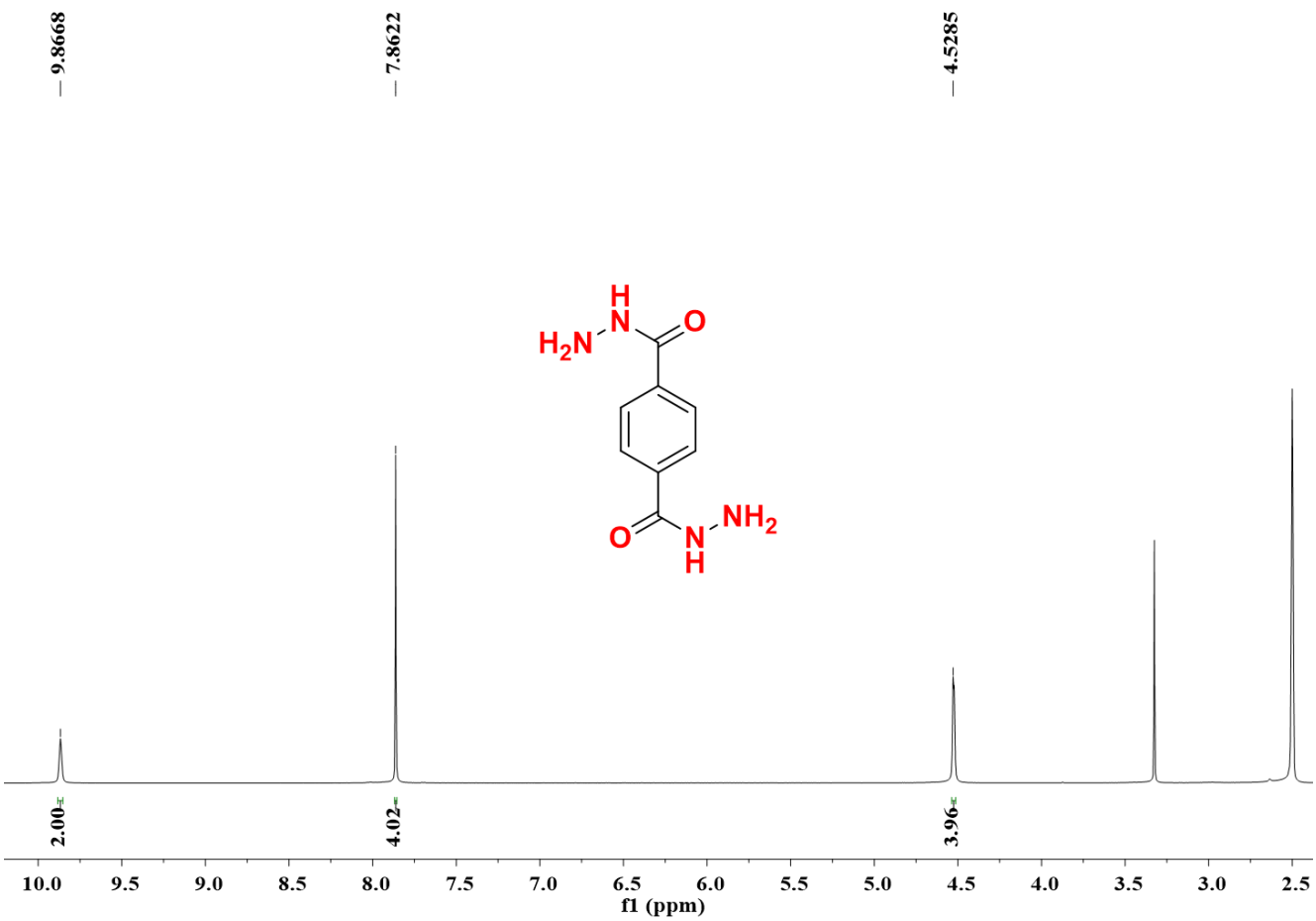


Figure S 51 $^{1}$H NMR spectrum of compound **2c** (DMSO-$d_6$, 500 MHz)

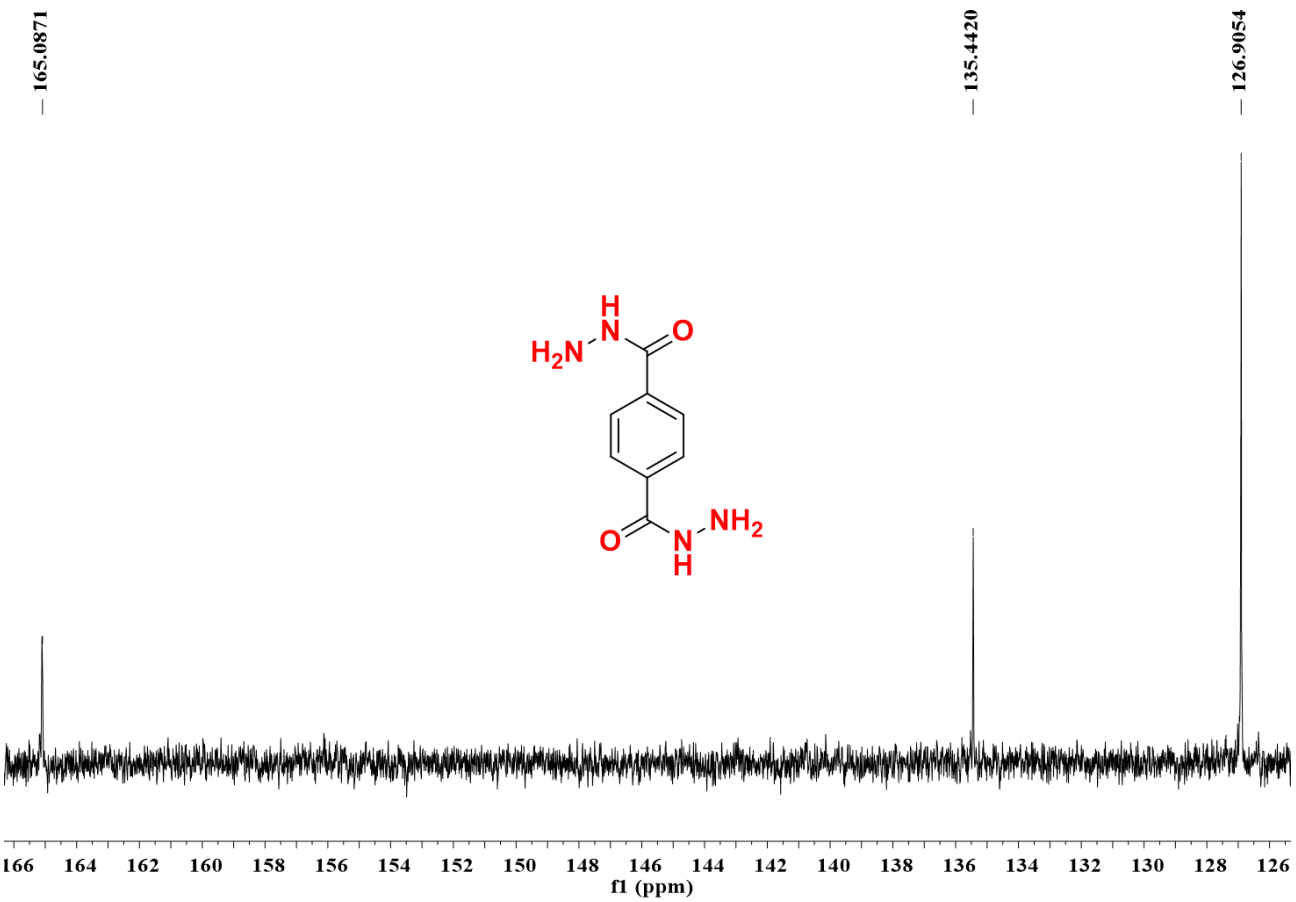


Figure S 52 $^{13}$C NMR spectrum of compound **2c** (DMSO-$d_6$, 125 MHz)

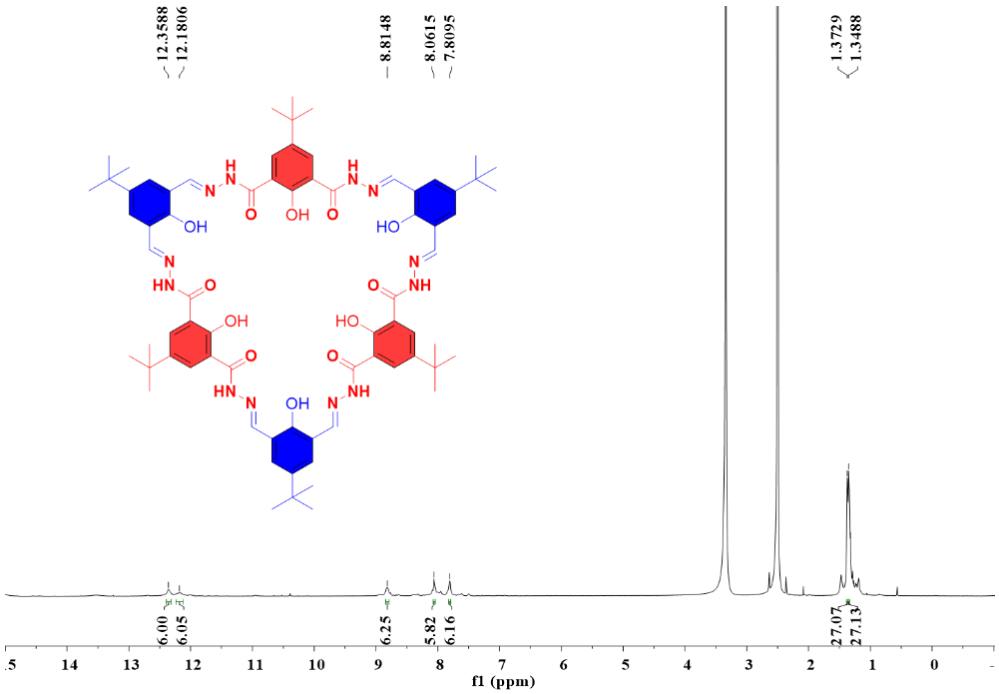


Figure S 53 $^{1}$H NMR spectrum of compound **6** (DMSO-$d_6$, 500 MHz, 5 mM, 2h)

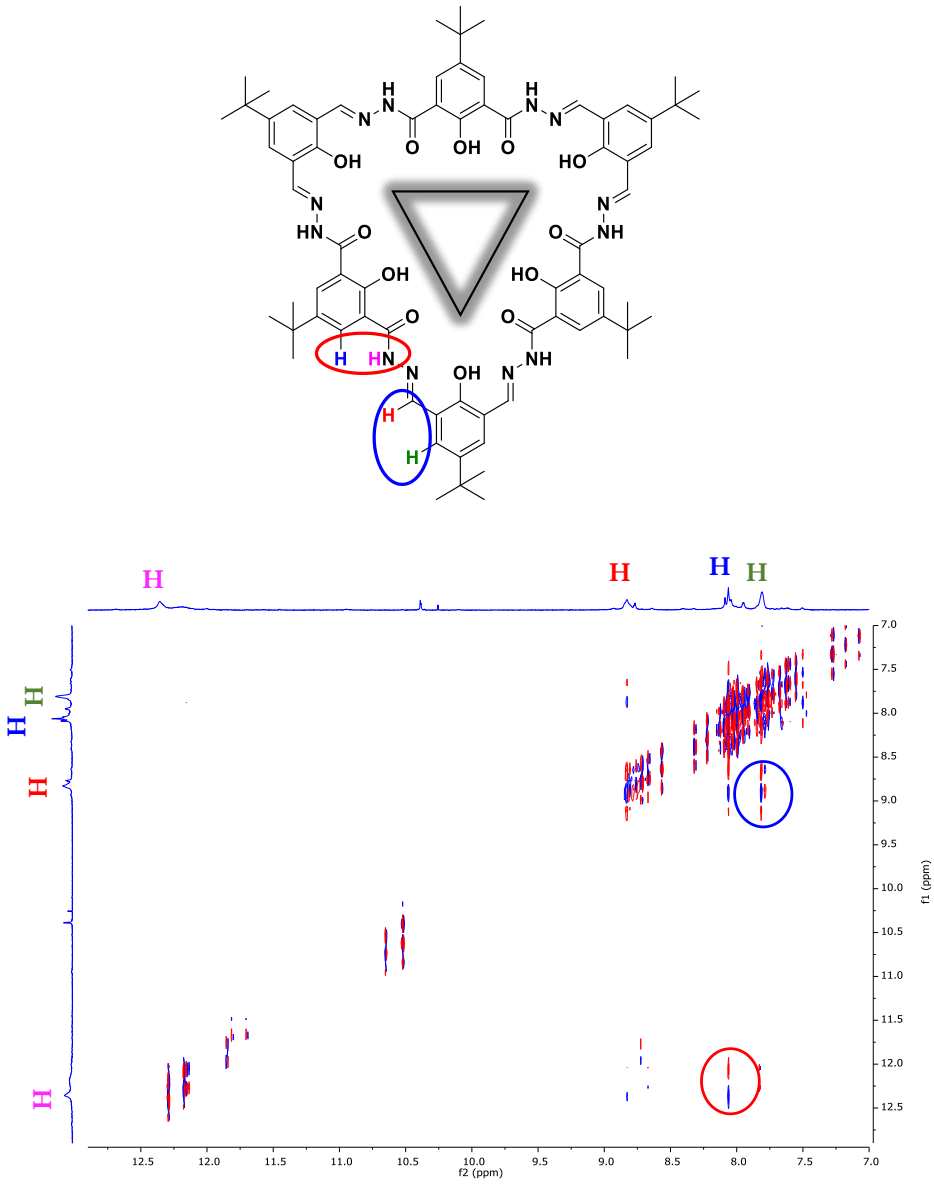


Figure S 54 NOESY spectrum of compound **6** (DMSO-$d_6$, 500 MHz, 7.5 mM)

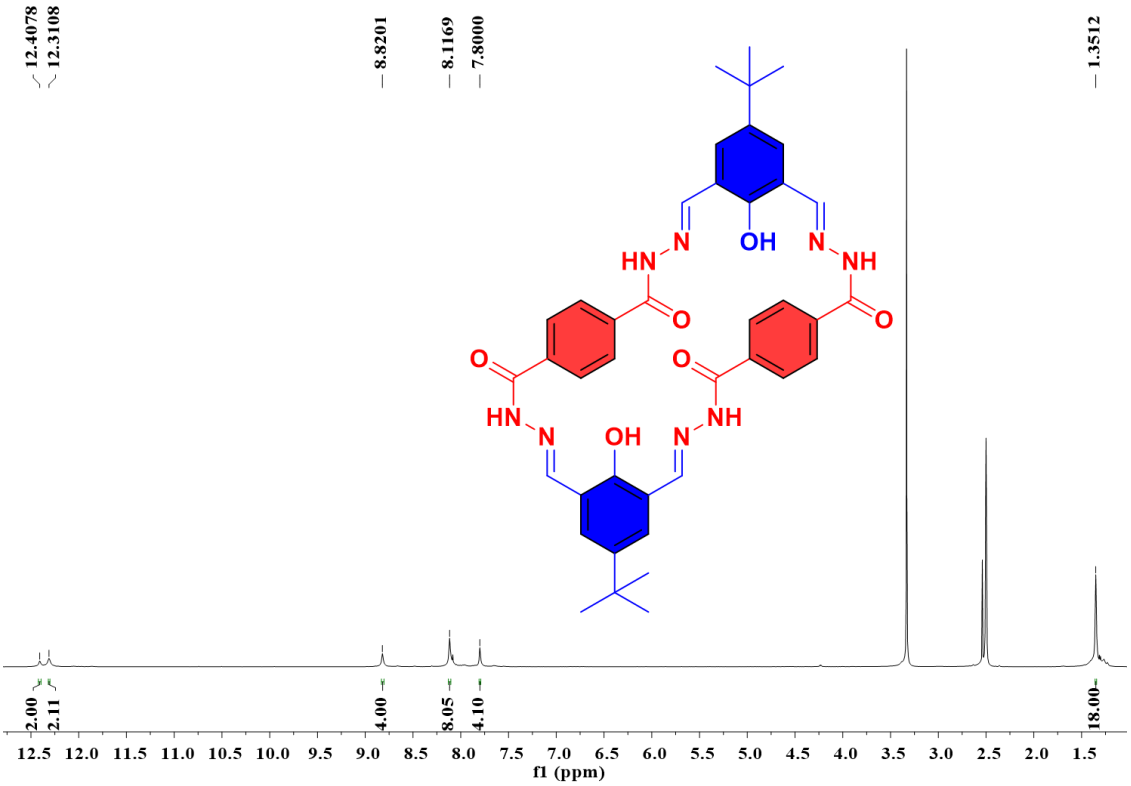


Figure S 55 $^{1}$H NMR spectrum of compound **7** (DMSO-$d_6$, 500 MHz, 5 mM, 3 days)

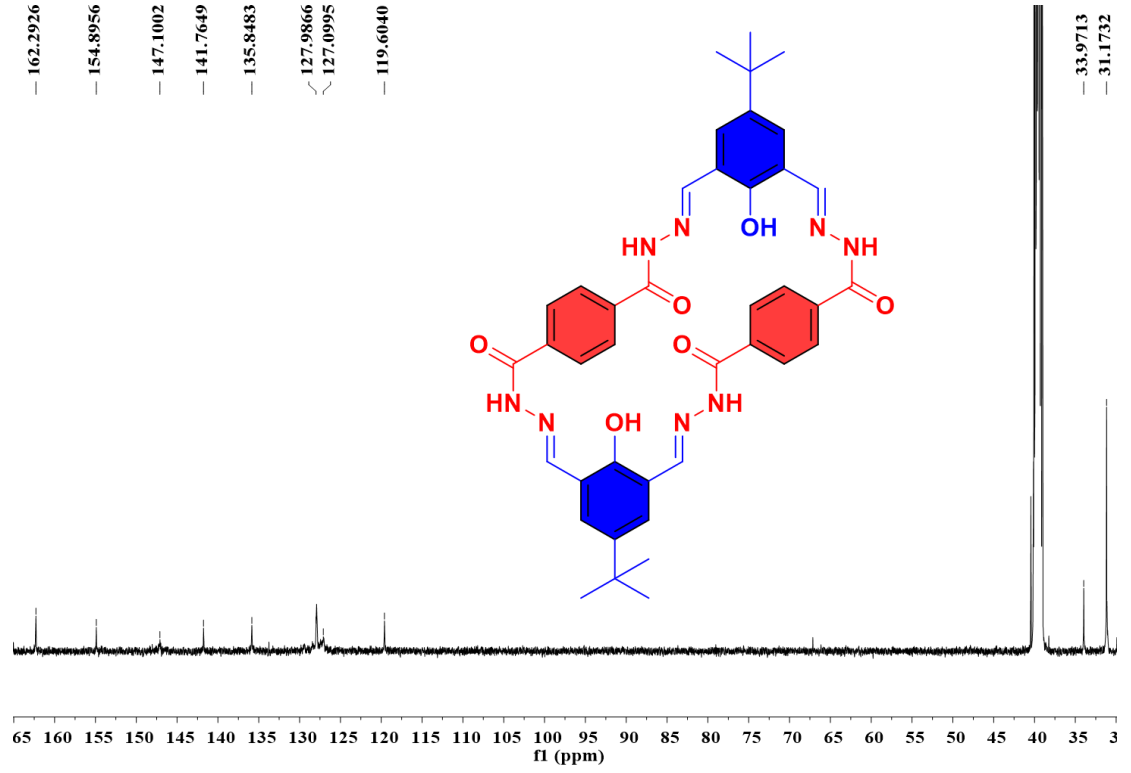


Figure S 56 $^{13}$C NMR spectrum of compound **7** (DMSO-$d_6$, 125 MHz, 5 mM, 3 days)

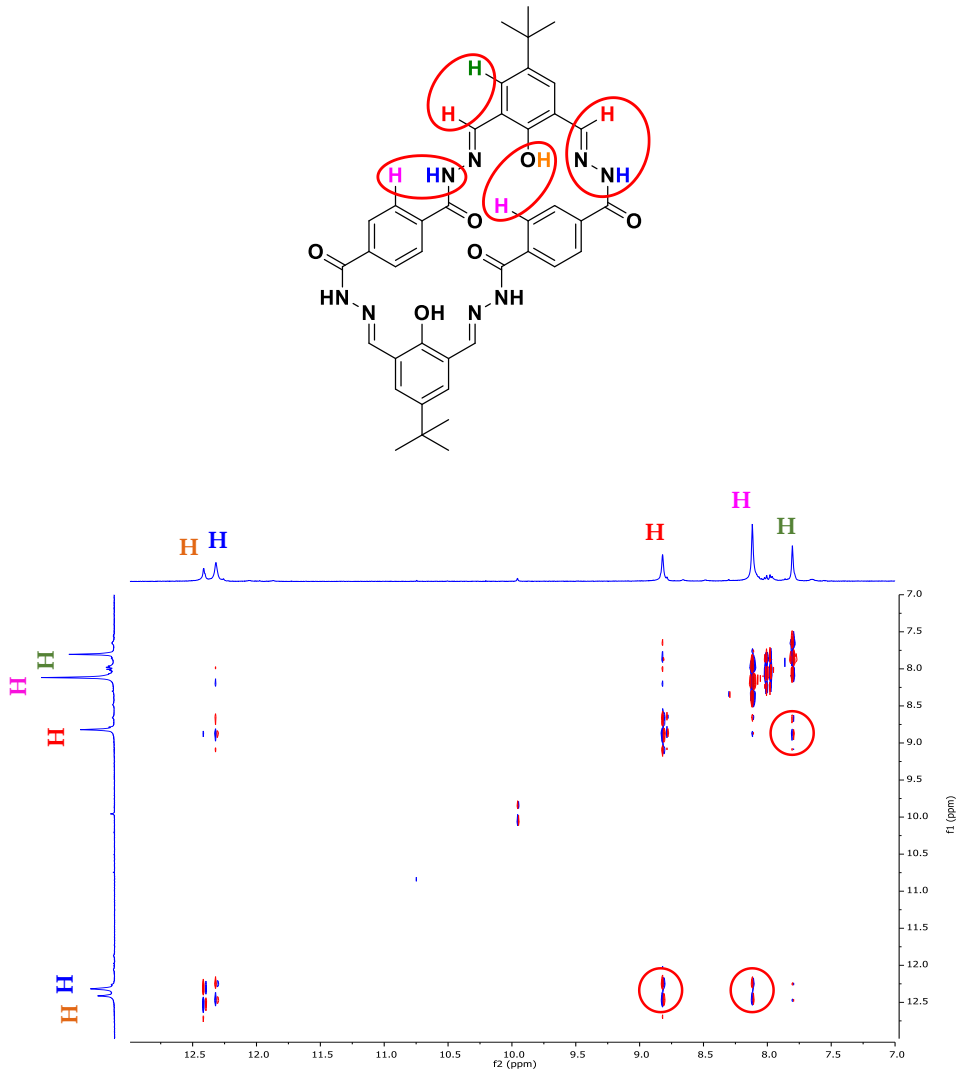


Figure S 57 NOESY spectrum of compound **7** (DMSO-$d_6$, 500 MHz, 5 mM, 3 days)

---

[1] A.G. Coman, A. Paun, C.C. Popescu, N.D. Hadade, A. Hanganu, A.M. Madalan, and Matache M., *Revue Roumaine de Chimie*, 2020, **65**, 109–114.
[2] W. Huang, S. Gou, D. Hu, and Q. Meng, *Synth Commun*, 2000, **30**, 1555–1561.
[3] L.F. Lindoy, *Synth*., 1998, **07**, 1029–1032.
[4] Z. Zhang, Y. Qu, M. Li, S. Wang, and J. Wang, *J. Chem. Eng. Data*, 2019, **64**, 4565–4579.
[5] K. Hu, D. Zhao, G. Wu, and J. Ma, *RSC Adv.*, 2017, **7**, 32989–33000.
[6] V.V. Korshak, L.S. Fedorova, and K.K. Mozgova, *Chem Heterocycl Compd.*, 1970, **3**, 776–778.
[7] R. Cavier, and R. Rips, R., *J Med Chem*, 1965, **8**, 706–708.